Acta Biomaterialia 185 (2024) 296–311

Contents lists available at ScienceDirect

Acta Biomaterialia

journal homepage: www.elsevier.com/locate/actbio

Full length article

Intermittent cyclic stretch of engineered ligaments drives hierarchical collagen fiber maturation in a dose- and organizational-dependent manner

Leia D. Troop[a], Jennifer L. Puetzer[a,b,*]

[a] Department of Biomedical Engineering, Virginia Commonwealth University, Richmond, VA 23284, United States
[b] Department of Orthopaedic Surgery, Virginia Commonwealth University, Richmond, VA 23284, United States

ARTICLE INFO

Article history:
Received 20 March 2024
Revised 10 July 2024
Accepted 11 July 2024
Available online 16 July 2024

Keywords:
Ligament
Tissue engineering
Cyclic load
Mechanobiology
Collagen

ABSTRACT

Hierarchical collagen fibers are the primary source of strength in tendons and ligaments; however, these fibers largely do not regenerate after injury or with repair, resulting in limited treatment options. We previously developed a static culture system that guides ACL fibroblasts to produce native-sized fibers and early fascicles by 6 weeks. These constructs are promising ligament replacements, but further maturation is needed. Mechanical cues are critical for development *in vivo* and in engineered tissues; however, the effect on larger fiber and fascicle formation is largely unknown. Our objective was to investigate whether intermittent cyclic stretch, mimicking rapid muscle activity, drives further maturation in our system to create stronger engineered replacements and to explore whether cyclic loading has differential effects on cells at different degrees of collagen organization to better inform engineered tissue maturation protocols. Constructs were loaded with an established intermittent cyclic loading regime at 5 or 10 % strain for up to 6 weeks and compared to static controls. Cyclic loading drove cells to increase hierarchical collagen organization, collagen crimp, and tissue tensile properties, ultimately producing constructs that matched or exceeded immature ACL properties. Further, the effect of loading on cells varied depending on degree of organization. Specifically, 10 % load drove early improvements in tensile properties and composition, while 5 % load was more beneficial later in culture, suggesting a shift in mechanotransduction. This study provides new insight into how cyclic loading affects cell-driven hierarchical fiber formation and maturation, which will help to develop better rehabilitation protocols and engineer stronger replacements.

Statement of significance

Collagen fibers are the primary source of strength and function in tendons and ligaments throughout the body. These fibers have limited regenerate after injury, with repair, and in engineered replacements, reducing treatment options. Cyclic load has been shown to improve fibril level alignment, but its effect at the larger fiber and fascicle length-scale is largely unknown. Here, we demonstrate intermittent cyclic loading increases cell-driven hierarchical fiber formation and tissue mechanics, producing engineered replacements with similar organization and mechanics as immature ACLs. This study provides new insight into how cyclic loading affects cell-driven fiber maturation. A better understanding of how mechanical cues regulate fiber formation will help to develop better engineered replacements and rehabilitation protocols to drive repair after injury.

1. Introduction

Tendons and ligaments are critical for movement and stability, providing the strength for load transfer from muscle-to-bone and bone-to-bone, respectively. Tendons and ligaments are able to transfer and withstand these loads primarily due to hierarchically organized and aligned collagen fibers that run the length of the tissue [1–4]. Cells produce these hierarchical fibers by assembling tropocollagen molecules into fibrils (10–300 nm diameter), fibers (>10 μm diameter), and fascicles (100s μm to mm diameter) [5–7]. Each of these hierarchical levels reinforce the structure as a whole [3,8–10]. This multiscale hierarchical structure, along with proteo-

* Corresponding author at: 70 S. Madison St, Engineering Research Building, Room 3327, Virginia Commonwealth University, Richmond, VA 23220, United States.
E-mail address: jlpuetzer@vcu.edu (J.L. Puetzer).

https://doi.org/10.1016/j.actbio.2024.07.025
1742-7061/

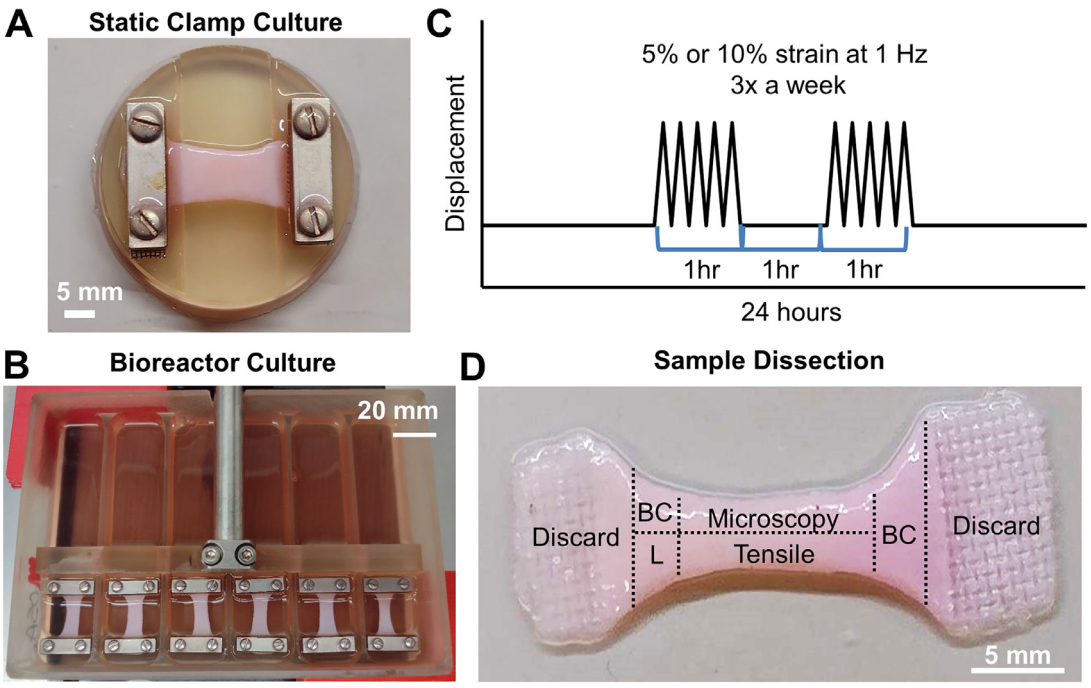

Fig. 1. Experimental setup with constructs either statically clamped or cyclically loaded at 5 or 10 % strain for up to 6 weeks. A) Static clamping culture device and B) bioreactor setup for cyclically loaded constructs. C) Depiction of intermittent loading regime. Constructs were loaded with an established loading regime, 3 times a week (MWF) for 1 hour on, 1 hour off, 1 hour on at 1 Hz and 5 % or 10 % strain. D) Depiction of tissue sectioning performed at each timepoint. Clamped regions were discarded and remaining tissue was allocated for biochemical composition (BC), lysyl oxidase activity (L), mechanical, and microscopy analysis.

glycans, collagen crosslinking and fiber crimp, provides tendons and ligaments with strong, non-linear, mechanical properties that are essential for long-term function [3,5,8–12]. The importance of these fibers to function are well understood, but replicating this hierarchical organization after injury or in engineered tissues remains a challenge [13,14].

Injuries to tendons and ligaments disrupt the collagen organization resulting in loss of function, pain, and decreased mobility [14,15]. Collagen fibers largely do not regenerate after injury or with repair, often resulting in unorganized scar tissue with reduced tissue function compared to healthy tissue [1,14]. There are more than 32 million tendon and ligament injuries per year in the United States [16] with limited repair options. In particular, the anterior cruciate ligament (ACL), which helps to stabilize the knee, is one of the most commonly injured ligaments resulting in an estimated 150,000 reconstructions each year in the US alone [17,18]. The current gold standards for ACL repair are autograft or allograft replacement. In addition to limited availability of donor tissue, these treatments have major drawbacks, including risk of donor site morbidity for autografts, immune response for allografts, and high risk of re-rupture [5,14–16,19–21]. More recently, devices facilitating partial repair such as the Arthrex repair kit or the Bridge-Enhanced ACL repair device have been approved for use, but these are limited by compatibility with specific injury patterns and have similar failure rates to traditional ACL repair [22–24]. Engineered replacements are promising alternatives, however, it remains a challenge to form the large hierarchically organized, crimped collagen fibers essential to long-term mechanical success [14,15].

Recently, we developed a novel culture system that guides ACL fibroblasts in unorganized high density collagen gels to develop hierarchically organized collagen fibers over 6 weeks of static culture [25,26]. Specifically, static boundary restraints (clamps) at the edge of the construct (Fig. 1A) restrict cellular contraction and guide cells to produce aligned fibrils by 2 weeks of culture, which mature into native-sized collagen fibers and larger collagen bundles or early fascicles by 4 and 6 weeks. These are some of the largest, most organized fibers produced to date *in vitro*; however, further maturation is needed for these constructs to serve as functional replacements.

Mechanical cues, including cyclic muscle activity, are critical for tissue development *in vivo* [1,5,27,28] and have been shown to drive maturation in engineered tissues *in vitro* [20,29–37]. In particular, intermittent cyclic loading at or below 5 % strain, which mirrors typical physiological strains for tendons and ligaments, is well established to improve fibril organization in engineered tendons and ligaments [1,20,28–36]; however the effect beyond the fibril level and on hierarchical fiber formation is largely unknown [1,13]. Further, the ACL, unlike tendons which typically experience a maximum tensile strain of 2–5 % [38,39], has been reported to experience up to 12 % strain [40] in each gait cycle, suggesting strain magnitudes above 5 % may be beneficial for ACL fibroblasts, particularly beyond the fibril level which is less understood [1,40,41]. Additionally, there are large variations in optimal loading conditions for engineered tissues, most likely due to differences in scaffold material and design, which ultimately alter how the applied load is translated to cells [38]. Our static culture system, which transitions from unorganized collagen at 0 weeks to aligned fibrils and fibers by 2 and 4 weeks, provides a means to explore how cells differentially respond to cyclic loading with different degrees of collagen organization. A better understanding of how cells respond to applied load at different levels of collagen organization could help to produce more uniform loading protocols across engineered systems and help to develop more optimal rehabilitation protocols.

The objective of this study was to investigate whether intermittent cyclic stretch, mimicking rapid muscle activity, could drive further maturation in our culture system. Additionally, we were interested in exploring whether 10 % strain drives improvements over 5 % strain in ACL fibroblast seeded constructs and whether cyclic loading had differential effects on cellular response when applied at different degrees of collagen organization. We hypoth-

esize that intermittent cyclic loading will improve hierarchical collagen organization, composition, and tissue tensile strength in a dose- and organizational-dependent manner, resulting in significantly stronger, functional ligament replacements.

2. Methods and materials

2.1. Cell isolation

Ligament fibroblasts and native samples were isolated from neonatal bovine as previously described [25,26,42]. Briefly, neonatal (1–3 day old) bovine legs were obtained from a slaughterhouse within 48 h of culling. The bovine cranial cruciate ligament (CCL), analogous to the human ACL and referred to as bovine ACL for the remainder of the manuscript, was aseptically isolated, diced, and digested for 15–18 h in 0.2 % collagenase. Cells were filtered, washed, counted, and frozen at 3 million cells/mL. Two separate isolations were performed, with each isolation having 3–4 donors pooled together. Prior to making constructs, cells were seeded at 2800 cells/cm^2 and expanded 1 passage in Dulbecco's Modified Eagle Medium (DMEM) media with 10 % fetal bovine serum (FBS), 1 % antibiotic/antimycotic, 50 µg/ml ascorbic acid, and 0.8 mM l-proline. Native samples used for image and composition analysis were isolated and stored as described in Section 2.5 and 2.7 at time of dissection.

2.2. Construct fabrication

High density, cell laden collagen gels were fabricated as previously described [25,26,42,43]. Briefly, type I collagen was extracted from an equal number of male and female Sprague-Dawley rat tail tendons (BIOIVT) and reconstituted at 30 mg/ml in a 0.1 % acetic acid solution [25,44]. To generate constructs, 2 mL of 30 mg/mL collagen was mixed with 0.5 mL of a working solution composed of 0.2 mL of 1x phosphate buffer saline (PBS), 0.25 mL of 10x PBS, and 0.05 mL of 1 N NaOH. This working solution raises the pH to 7 to initiate collagen gelation and the osmolarity to 300 mOsm [43–45]. This solution was then immediately mixed with 0.5 mL of cells suspended in media at 30 million cells/mL, ensuring cells were spread throughout the gel, cast into a 1.5 mm thick sheet gel, and allowed to set for 1 hour at 37 °C. The resulting 3 mL sheet gels, at 20 mg/mL collagen and 5×10^6 cells/mL, were cut into rectangles (8 × 30 mm) and divided between groups for culture. A different collagen stock was used for each sheet gel, with each sheet gel yielding 4–6 rectangular constructs. These constructs were distributed across experimental groups and time points. Thus, N refers to individual constructs produced from different collagen stocks and cell expansions.

2.3. Culture conditions and mechanical stimulation

One day after fabrication, static constructs were clamped into our culture device (Fig. 1A) as previously described [25,26,43], while loaded constructs were clamped into a modified CellScale tensile bioreactor (Fig. 1B), with both static and loaded constructs having a 20 mm gauge length between clamps. Static constructs were cultured clamped to guide hierarchical fiber formation, with no additional applied strain, as in previous studies [25,26,43]. Loaded constructs were stimulated with an intermittent cyclic loading regime (Fig. 1C) established to generate matrix turnover and anabolic cellular response in engineered tissues [42,45–48]. Specifically, constructs were loaded with either 5 % or 10 % strain at 1 Hz for 1 hour on, 1 hour off, 1 hour on, 3x a week (Monday, Wednesday, Friday) to evaluate the effect of cyclic loading magnitude (Fig. 1C). Further, 1 Hz is an established loading frequency for engineered ligaments [42,45,47,49] and mirrors physiological loading [41,50,51]. Culture media was the same as that used for cell expansion. Conditional media changes were performed immediately prior to loading by replacing half of the media during each media change throughout culture every 2–3 days [42].

2.4. Post-culture analysis

Time points were taken at 0, 2, 4, and 6 weeks, with 0-week constructs taken out of culture 24 h after 1 loading cycle. At each time point, 6–10 constructs per group were removed from culture, weighed, photographed, and sectioned for analysis of collagen hierarchical organization, composition, and tissue tensile properties as previously described (Fig. 1D) [27,31,45,52]. Due to significant contraction later in culture, not all sections for analysis could be obtained from a single loaded construct, thus a greater number of constructs had to be produced for loaded groups ($N = 10$) compared to control static constructs ($N = 6$). To track changes in contraction, construct percent weight and percent area were determined at each time point. Percent weight was calculated by comparing whole construct wet weights to respective 0 week constructs. Percent area was determined by measuring construct surface area between the clamps in photographs taken at each time point using FIJI (NIH) and comparing to respective 0 week constructs, as previously described [26,42].

2.5. Hierarchical collagen organization analysis

Hierarchical collagen organization at the fibril (<1 µm), fiber (1–100 µm), and fascicle (>100 µm) length-scales were performed via scanning electron microscopy (SEM), confocal reflectance, and picrosirius red staining as previously reported [26,42,43]. Briefly, length-long sections of constructs and neonatal bovine ACLs were fixed in 10 % formalin and stored in 70 % ethanol. A total of 5–7 constructs per time point and condition and 5 neonatal ACLs were analyzed via confocal reflectance. Following confocal analysis, a subset of 6 week constructs and neonatal ACLs were processed for SEM ($N = 3$) and picrosirius red staining ($N = 3$).

2.5.1. Confocal reflectance imaging and analysis

Confocal imaging for fiber level analysis was performed with a Zeiss LSM 980 microscope and Plan-Apochromat 20x/1.2 objective as previously described [25,37,45,53]. Briefly, a 405 nm laser was used to visualize collagen by capturing reflectance through a 27 µm pinhole at 400–465 nm, while simultaneously a 488 nm laser was used to capture auto-fluorescence of cells at 509–571 nm. Five to eight representative 2D images were taken across the length of each construct and 3D images of 6 week constructs were obtained via Z-stacks with less than 1 µm step size and 18 - 22 µm depth. Z-stacks were visualized with the FIJI 3D viewer plugin.

Confocal 2D images of constructs and native ACLs were analyzed using a custom Fast Fourier transform (FFT) based MATLAB code to determine degree of collagen alignment and fiber diameter as previously described [53]. Collagen alignment was scored using an alignment index, where 1 is unorganized and 4.5 is completely aligned, and average fiber diameter was the average frequency pattern detected in each image by FFT measurements [53]. Accuracy of FFT measurements were confirmed by manual fiber measurements made using FIJI. Five to eight representative images taken across each construct were analyzed and averaged to determine alignment and diameter for each construct. The reported alignment and diameter values are the average and standard error of construct values ($N = 5$–7 for constructs, $N = 5$ for neonatal ACL).

2.5.2. SEM imaging and analysis

SEM analysis of fibril level (<1 μm scale) organization was performed on 6 week constructs and neonatal bovine ACL with a Hitachi SU-70 FE-SEM as previously described [26,42,43]. Briefly, samples were dried via critical point drying and coated with 0.025–0.035 kAngstroms Platinum. Samples were imaged at a working distance of 10 mm, with 5 kV, at 10,000X and 50,000X magnification, with at least 6 images taken per sample. Images at 50,000X were analyzed to determine alignment and fibril diameter. Degree of alignment was measured by determining dispersion using the FIJI directionality function as previously described [26]. Dispersion values were obtained for 6–8 images per sample and averaged to determine average construct dispersion. The reported dispersion values are the average of construct values ($N = 3$ for constructs and native ACL). To determine fibril diameter a total of 20 fibrils per image were measured using FIJI (total 120 fibrils per construct) and pooled to determine average fibril diameter for each construct [43]. All fibril diameters from $N = 3$ samples ($n = 360$) were pooled for violin plots to visualize spread of diameters at 6 weeks. To validate manual measurements, the average fibril diameter of images were confirmed via DiameterJ Segment and DiameterJ 1–018 FIJI plugins, however manual measurements are reported to retain insight in fibril diameter dispersion. For statistical analysis of fibril diameter, 120 fibril diameters per sample were averaged to compare construct averages at 6 weeks ($N = 3$ for constructs and native ACL).

2.5.3. Polarized picrosirius red imaging

Histological analysis was performed to observe fascicle level (> 100 μm scale) organization and crimp as previously described [25,26,42,43]. Briefly, fixed constructs ($N = 3$) and neonatal bovine ACL ($N = 3$) were embedded in paraffin, sectioned, and stained with picrosirius red. Constructs were imaged with a Nikon Eclipse Ts2R inverted microscope and Nikon Pan Fluor 10x/0.30 OFN25 Ph1 DLL objective in linear polarized light at 10, 20, and 30x magnification. To evaluate crimp period length, 5 images per construct were obtained at 20x magnification and FIJI Plot Profile analysis tool was used to record brightness values across 3 random fibers per image, ensuring the line covered 5–8 crimp formations per fibers (resulting in 16–20 crimp measurements per image). Crimp period length was defined as the distance between peaks in brightness, similar to previous studies [54–58]. Measurements were pooled across all images for each construct ($n = 86–100$) to determine average crimp length per construct ($N = 3$ for engineered and native ACL). Static controls were not analyzed due to inconsistent and limited crimp formation.

2.6. Mechanical analysis

Tensile tests were performed as previously described [43,53]. Briefly, samples ($N = 6–8$) were collected along the length of each construct, frozen for storage, thawed in PBS with EDTA-free protease inhibitor prior to testing, measured, and stretched to failure with a BOSE ElectroForce 3200 System equipped with a 250 g load cell. Samples were secured using serrated grips (TA electroforce 332368-0010) and loaded at a strain rate of 0.75 % strain/second to failure, assuming quasi-static load and ensuring failure between the grips, similar to previous studies [25,26,37,42,43,45,53]. While sample dimensions decreased with time in culture as constructs contracted, samples maintained relatively similar dimensions across conditions at each timepoint with a grip-to-grip lengths of ~3–4 mm, a sample width of ~1–2 mm, sample thickness of ~0.3–1 mm (see **Supplemental Table 1** for average dimensions across time points). Tensile properties were determined via a previously developed linear regression-based MATLAB code [42]. Briefly, the toe and elastic moduli were determined by individually fitting a linear regression to the stress-strain curve in each region, ensuring an $r^2 > 0.999$, and the transition point was defined as where these two linear regressions intersected. The maximum point on the stress-strain curve was used to determine the ultimate tensile strength (UTS) and strain at failure. The toe and elastic moduli are more accurately the apparent tangent moduli of the stress-strain curve, however, for simplicity they will be referred to as the toe and elastic modulus throughout the manuscript.

2.7. Compositional analysis

Compositional analysis for DNA, glycosaminoglycan (GAG), and collagen content were performed as previously described [25,26,42,43]. Briefly, two sections per construct were taken for compositional analysis (Fig. 1D) and the values were averaged to determine composition for each construct. Construct sections and neonatal bovine ACL samples were weighed wet (WW), frozen, lyophilized, weighed dry (DW), and digested in 1.25 mg/ml papain solution at 60 °C for 15–16 h ($N = 6–8$). DNA, GAG, and collagen were determined via a modified Quant-iT PicoGreen dsDNA assay kit (Invitrogen), 1,9-dimethylmethylene blue (DMMB) assay at pH 1.5 [59], and a modified hydroxyproline (hypro) assay [60]. Constructs from each experimental group retained similar percent wet weight throughout culture, so DNA, GAG, and hydroxyproline are reported normalized to sample wet weight. To evaluate whether composition was similar across constructs, samples taken from each side of the construct were compared. Comparisons are reported as the composition in the sample closest to the moving pull arm of the bioreactor to the composition of the sample closest to the unmoving, static clamp of the bioreactor (**Supplemental Fig 1A**).

To determine LOX activity in constructs, separate sections taken from alternating sides of the constructs (Fig. 1D, $N = 5–6$) were placed in a 6 M Urea 10 mM Tris–HCl solution at pH 7.4 with 1 % protease inhibitor at each time point and frozen at −80 °C. A fluorometric LOX activity assay (Abcam, ab112139) was used to determine arbitrary units (A.U.) of LOX activity. The assay was run according to manufacturer protocol with recombinant LOXL2 (R&D Systems) used as a positive control and results normalized to sample DNA determined via the Quant-iT Picogreen dsDNA assay, as the LOX enzyme is produced and released from cells.

2.8. Acellular constructs

To determine if load alone, rather than cellular response to load, drives collagen organization, acellular constructs were cultured in the same manner as cell-seeded constructs. Acellular constructs were produced as described above, however, instead of cell-seeded media being added to the collagen mixture, media alone was mixed into the collagen solution to produce 20 mg/ml constructs. Acellular constructs were cultured statically clamped, or with 5 % or 10 % intermittent cyclic loading for up to 6 weeks as described above. At 0 and 6 weeks, constructs were removed from culture ($N = 4–6$) and sectioned the same as cell-seeded constructs for analysis of collagen organization, tissue tensile strength, and composition (Fig. 1D). Specifically, collagen organization was assessed by confocal reflectance, tensile properties were assessed via tensile tests to failure (see **Supplemental Table 2** for test sample dimensions), and collagen concentration was assessed as a measure of composition, all done according to methods above for cell-seeded constructs.

2.9. Statistics

For image and compositional analysis, where multiple measurements per construct were taken, measurements were pooled and

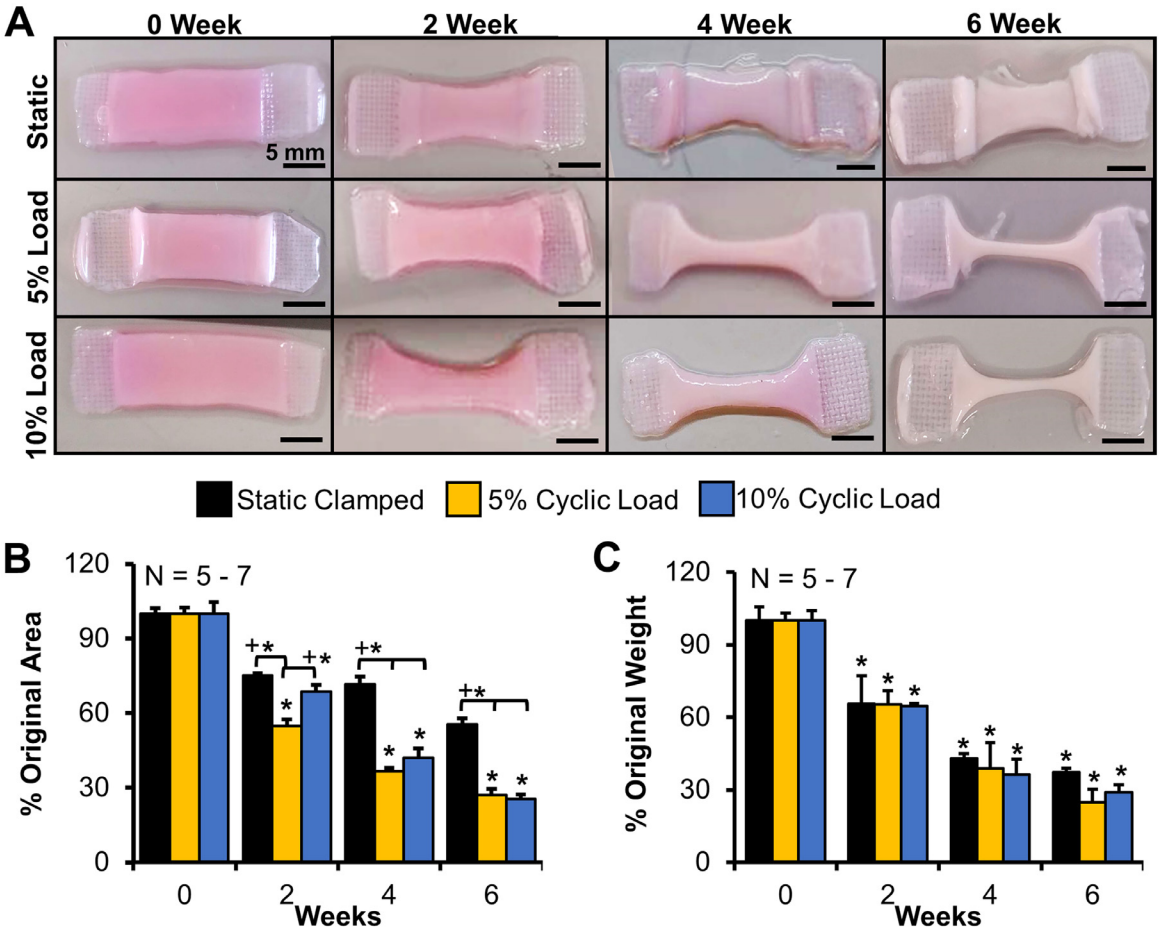

Fig. 2. Loading appeared to increase construct contraction, but construct wet weight remained similar to controls. A) Photographs of representative constructs at each time point, B) percent area and C) percentage wet weight throughout culture compared to respective 0 week constructs. Scale bar = 5 mm, Data shown as mean ± S.E.M., Significance compared to *0 week or +bracket group ($p < 0.05$).

averaged to determine an overall value for the construct and statistical analysis was performed using construct averages. For all data, Shapiro-Wilk tests were used to confirm normality within each group. Following confirmation of normality, data were analyzed via 2-way ANOVA and Tukey's post-hoc analysis with $p < 0.05$ as significant (SigmaPlot 14). The two effects investigated were culture condition and time in culture. Since fibril dispersion, fibril diameter, and crimp length data were only collected at 6 weeks, this data was analyzed via 1- way ANOVA. All data are expressed as mean ± standard error (S.E.M.).

3. Results

3.1. Gross morphology

Gross inspection revealed all constructs contracted with time in culture, with both 5 and 10 % load constructs appearing to have accelerated and increased contraction compared to static constructs by 4 weeks (Fig. 2A). Percent area measurements confirmed this observation, with loaded constructs having a significantly lower percent area compared to static controls starting by 2 weeks (Fig. 2B). However, interestingly, percent weight measurements, based on the wet weight of constructs, revealed all constructs contracted similarly with time in culture to 30–40 % their original weight (Fig. 2C). Loading did not significantly affect percent weight compared to static constructs, suggesting that while there were differences in surface area reduction, loaded and static samples retained similar mass.

3.2. Hierarchical collagen organization

Confocal reflectance analysis revealed all groups guided cells in unorganized collagen at 0 weeks to produce aligned collagen fibrils by 2 weeks and larger fibers by 4 and 6 weeks, similar to previous studies (Fig. 3A) [25,26,43]. Loading accelerated fiber development, with collagen fibers in both 5 and 10 % load constructs appearing larger and more organized by 4 and 6 weeks, similar to neonatal bovine ACL. In addition to organization, loaded constructs appeared to have developed early crimp by 2 weeks, which appeared more uniform and regularly spaced by 6 weeks (Fig. 3A, arrows). Three-dimensional reconstructions of 6 week constructs further confirmed loaded constructs developed more clearly defined collagen fibers and increased crimp compared to static constructs, with 10 % load constructs appearing to have larger, more organized collagen bundles or early fascicle formations compared to 5 % (Fig. 3A, Z-stacks).

Analysis of confocal images revealed that all groups had significantly improved alignment by 2 weeks, matching neonatal bovine ACL alignment (Fig. 3B). Loading further significantly improved collagen alignment over static controls and native tissue by 4 and 6 weeks, however there were no significant differences in alignment between 5 % and 10 % load constructs. Average collagen fiber diameter also significantly improved for all groups with time in culture, with loading further improving fiber diameter in a dose-dependent manner. Both 5 and 10 % load produced significantly increased fiber diameters compared to static constructs by 4 weeks, which were no longer significantly different from neonatal diame-

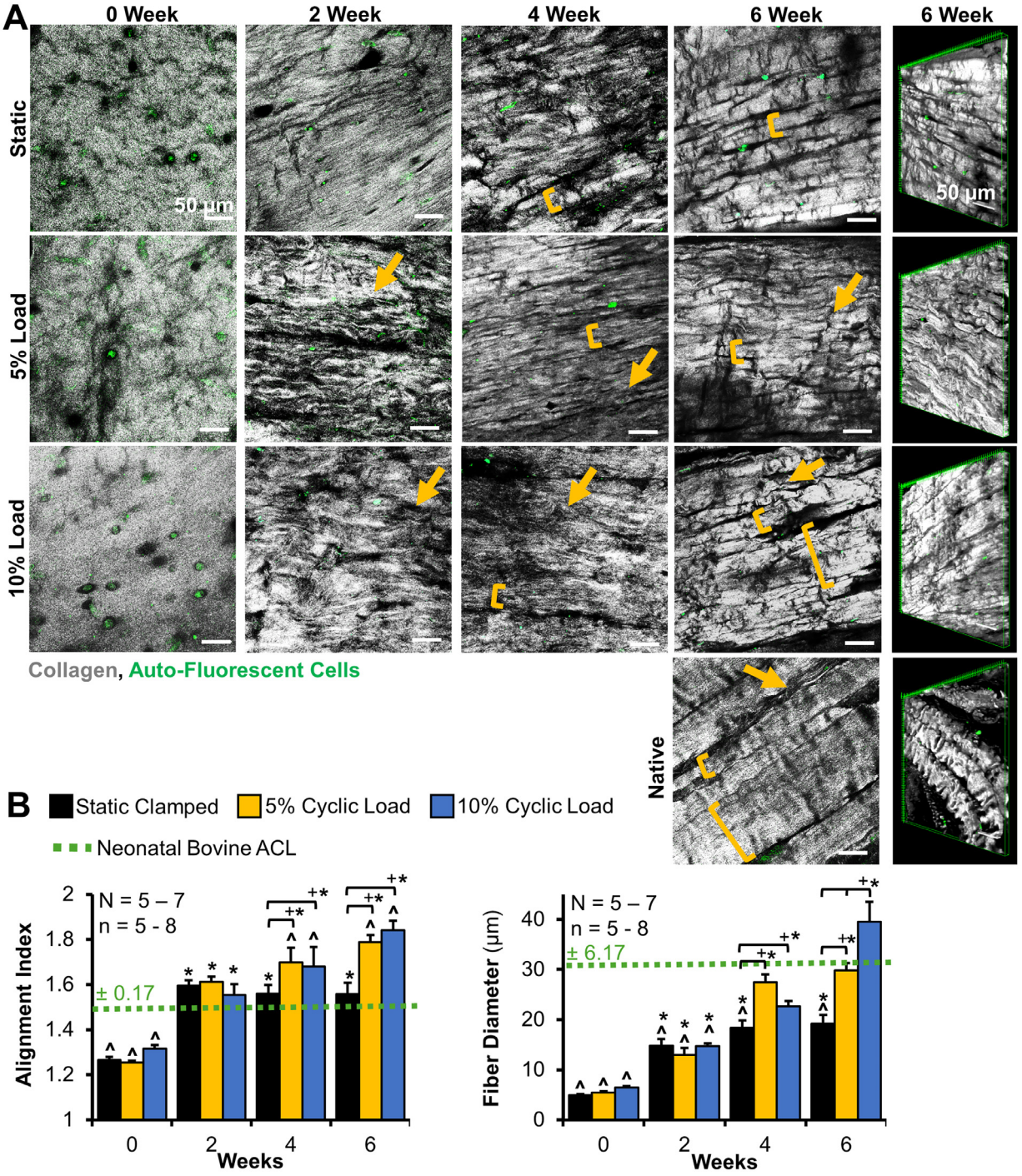

Fig. 3. Loading increased fiber development in a dose-dependent fashion. A) Confocal reflectance revealed constructs develop aligned fibrils at 2 weeks, and larger fibers by 4 weeks (brackets), with loading producing increased fiber and fascicle formation (larger brackets) and crimp formation (arrows). Grey = collagen, green = cellular autofluorescence. scale bar = 50 μm. B) Degree of collagen alignment (reported via alignment index where 1 is unorganized, 4.5 is perfectly aligned) and average collagen fiber diameter determined via a FFT based image analysis. 5–8 images per construct were averaged to determine construct values, with 5–7 constructs analyzed per time point and 5 native tissues analyzed. Data shown as mean ± S.E.M., Significant difference compared to *0 week, ^native, or +bracket group ($p < 0.05$).

ters. By 6 weeks, 10 % load constructs had significantly larger fibers compared to 5 % load and static constructs, reaching an average diameter of 38.9 ± 2.8 μm (Fig. 3B).

Similar to fiber level organization, SEM analysis revealed increased organization at the fibril level (<1 μm length-scale) in loaded constructs by 6 weeks (Fig. 4). Both 5 and 10 % load appeared to drive increased alignment of fibrils compared to static controls, as well as compaction of fibrils into larger bundles similar to neonatal tissue (Fig. 4A). Fibril banding was observed in engineered constructs at 6 weeks, but was less pronounced than that observed in native tissue, similar to previous studies [25]. Image analysis confirmed that by 6 weeks, 5 % and 10 % load constructs had significantly decreased degrees of dispersion (*i.e.* increased alignment) compared to static controls (Fig. 4B). Further, measurements of fibril diameter revealed loaded constructs had significantly larger fibril diameters than static controls at 6 weeks, with 10 % load constructs reaching average neonatal ACL diameters (~58 nm) and having significantly larger fibrils compared to

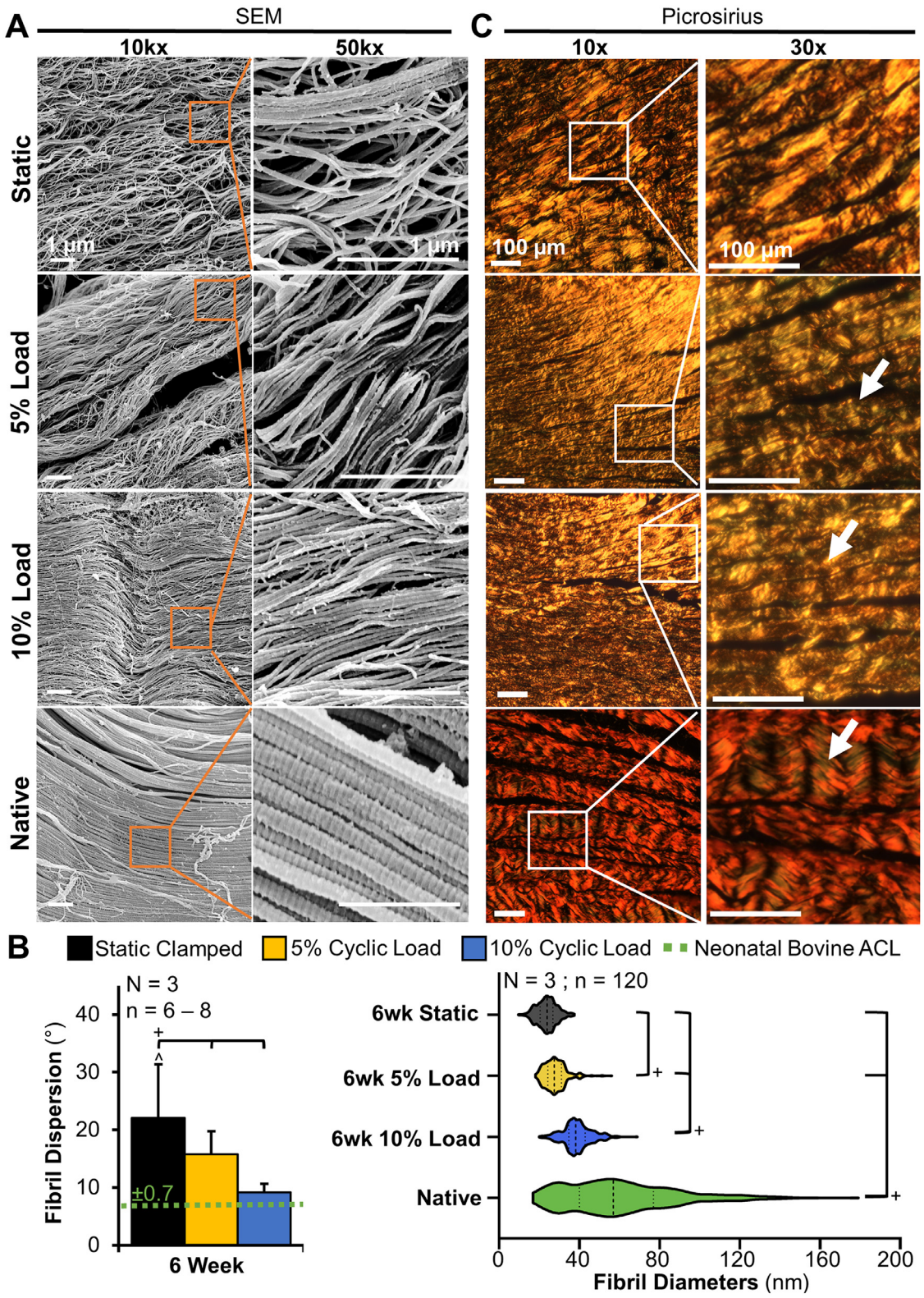

Fig. 4. Loading increased fibril and fascicle formation in a dose-dependent fashion. A) SEM images of 6-week constructs to assess fibril length-scale organization (scale bar = 1 µm), and B) analysis of SEM images to determine fibril dispersion (lower dispersion indicating increased alignment), and fibril diameter of 6 week constructs and neonatal bovine ACL. For dispersion, 6–8 images per construct were averaged to determine construct average ($N = 3$ for constructs and native ACL). For fibril diameters, 20 fibrils per image were measured (total 120 fibrils per construct) and pooled to determine average fibril diameter for each construct. All fibril diameters from $N = 3$ constructs were pooled ($n = 360$) to visualize spread of fibril diameters at 6 weeks. Data shown as mean ± S.E.M., Significance compared to ^native tissue or +bracket group ($p < 0.05$). C) Fascicle length-scale organization at 6 weeks evaluated by picrosirius red staining imaged with polarized light ($N = 3$, scale bar = 100 µm). Loading contributed to enhanced fascicle formation and crimp formation (arrows).

Table 1
Average crimp period length.

	Crimp Period (μm) 6 weeks
5 % Cyclic Load	19.7 ± 1.7 [a]
10 % Cyclic Load	28.5 ± 2.1 [b]
Neonatal ACL	36.7 ± 2.8

Values are Mean ± S.E.M. Crimp period was determined by averaging 85–100 crimp periods per construct (16–20 crimp periods per image, 5 polarized picrosirius red images per construct), with $N = 3$ constructs and native samples analyzed.
[a] Significance compared to neonatal bovine ACL group ($p < 0.05$).
[b] Significance compared to 5 % load group ($p < 0.05$).

5 % load constructs. Further, both loaded groups became more heterogeneous with a wide range of fibril sizes, more similar to native tissue.

Polarized picrosirius red analysis of the fascicle length-scale (>100 μm length-scale) further confirmed loading drove improvements in hierarchical collagen organization (Fig. 4C). Low magnification imaging (10x images) demonstrated loaded constructs had larger, more compact collagen bundles, indicative of early fascicle formation, compared to static controls. Higher level magnification (30x images) revealed 5 % and 10 % load constructs qualitatively had increased crimp formation compared to static controls, with 10 % load constructs appearing to have more pronounced, regularly spaced crimps than that of 5 %. Image analysis of crimp length confirmed 10 % load constructs had increased crimp period compared to 5 % load constructs, ultimately having an average crimp period which was not significantly different from neonatal ACL (Table 1). Collectively, intermittent cyclic loading drove accelerated and increased hierarchical fiber formation, with 10 % load producing regular crimps as well as increased fibril and fiber diameters that matched or exceeded neonatal bovine ACL.

3.3. Tissue mechanical properties

Mirroring improvements in organization, all constructs had significant improvements in tensile properties with time in culture (Fig. 5). Interestingly, despite 10 % load constructs having improved hierarchical fiber formation, only 5 % load constructs had improved elastic tensile properties over static controls by 6 weeks, with a significant increase in elastic modulus over static and 10 % load groups at 6 weeks (Fig. 5A). Ultimately 5 % load constructs had an elastic modulus of 3.5 ± 0.72 MPa at 6 weeks, surpassing reported immature 1 week old bovine ACL values (1–3 MPa [61]). Similarly, all constructs had improved UTS by 6 weeks. While 10 % load constructs had continual improvement in tensile properties with time in culture and significantly higher elastic modulus and UTS at 4 weeks compared to 5 % constructs, they had no significant differences in elastic modulus compared to static controls throughout culture, and a significantly lower UTS compared static controls by 6 weeks (Fig 5A). Both 5 % and 10 % groups had decreased strain at failure compared to static samples by 6 weeks, suggesting increased maturation and alignment of collagen fibers.

Despite 5 % load only producing significant increases in elastic properties over static controls, both 5 % and 10 % load constructs had significant improvements in toe region properties (Fig. 5B), with 5 % and 10 % groups having a 2.5- and 3.5-fold improvement in toe modulus over static constructs, respectively. Further, 10 % load constructs had accelerated improvements, with significant increases in toe modulus and transition stress by 4 weeks compared to static and 5 % load constructs, with no significant changes in transition strain.

3.4. Matrix composition and LOX activity

With time in culture, all constructs had a significant increase in DNA, GAG, and collagen concentration (normalized to wet weight and dry weight), with the effect of loading on composition varying with time in culture and degree of collagen organization (Fig. 6, **Supplemental Fig. 2** for dry weight normalizations). Despite all groups having similar decreases in percent wet weight (Fig. 2C), loading appeared to increase cell proliferation resulting in significant increases in DNA normalized to wet weight at 2 and 4 weeks for both 5 and 10 % load compared to controls, but this effect was lost by 6 weeks when all groups reached neonatal bovine ACL concentrations (Fig. 6). Interestingly, both load groups had a significant increase in GAG concentration at 0 weeks after just one loading cyclic, compared to static samples, and 10 % load constructs had a further significant increase in GAG accumulation at 2 and 4 weeks (Fig. 6). However, by 6 weeks, all treatment groups had similar levels of GAGs, with both load groups leveling off at neonatal ACL concentrations. Collagen content represented by hydroxyproline, decreased in 10 % load samples compared to static controls after one loading cycle and decreased in 5 % load samples at 2 weeks compared to static controls, indicating that the cells may have initially been breaking down collagen in response to load. By 4 weeks, this trend was reversed, with both load groups increasing collagen concentration to static control levels, with 5 % cyclic load constructs accumulating 2-fold more collagen than 10 % load constructs. By 6 weeks, 5 % load constructs reached neonatal bovine ACL collagen concentrations and had a significant 2-fold increase over static and 10 % load groups (Fig 6, **Supplemental Fig 2C**). No significant differences were found when comparing the DNA, GAG, and collagen concentrations obtained on each side of the constructs at 0 and 6 weeks, suggesting similar cellular response across the length of the construct (**Supplemental Fig 1C**). LOX activity was significantly increased by both 5 and 10 % load by 6 weeks (Fig. 6). Interestingly, LOX activity only increased for 10 % load constructs at 0 weeks after one loading cycle in unorganized collagen gels, and after 6 weeks of culture once aligned fibers had formed. Further, while 5 % load significantly increased LOX activity at 4 and 6 weeks, 10 % load constructs had a 2-fold increase over 5 % load constructs by 6 weeks.

3.5. Acellular constructs

Acellular constructs were also cultured for up to 6 weeks to determine if stretching of collagen gels alone, rather than cellular response to load, drives construct maturation. All acellular constructs had no contraction and no change in percent weight by 6 weeks (Fig. 7A). Likewise, static controls and loaded acellular constructs had no fibril alignment or larger fiber organization by 6 weeks (Fig. 7B). Constructs remained unorganized throughout culture. Further, there was no accumulation or significant loss of collagen in any treatment group (Fig. 7C) and no improvements in tissue tensile properties (Fig. 7D and **Supplemental Figure 3**). Collectively, this data suggests that any improvements in organization and tissue tensile properties were due to cellular response to load and not induced organization from stretching of the collagen gels alone.

4. Discussion

Collectively, this study demonstrates intermittent cyclic loading increases hierarchical collagen organization, crimp formation, and tissue tensile properties. Both 5 and 10 % load accelerated and increased hierarchical collagen fiber formation in a dose-dependent fashion, producing fibrils and fibers that matched neonatal bovine diameters by 6 weeks. Further, both magnitudes

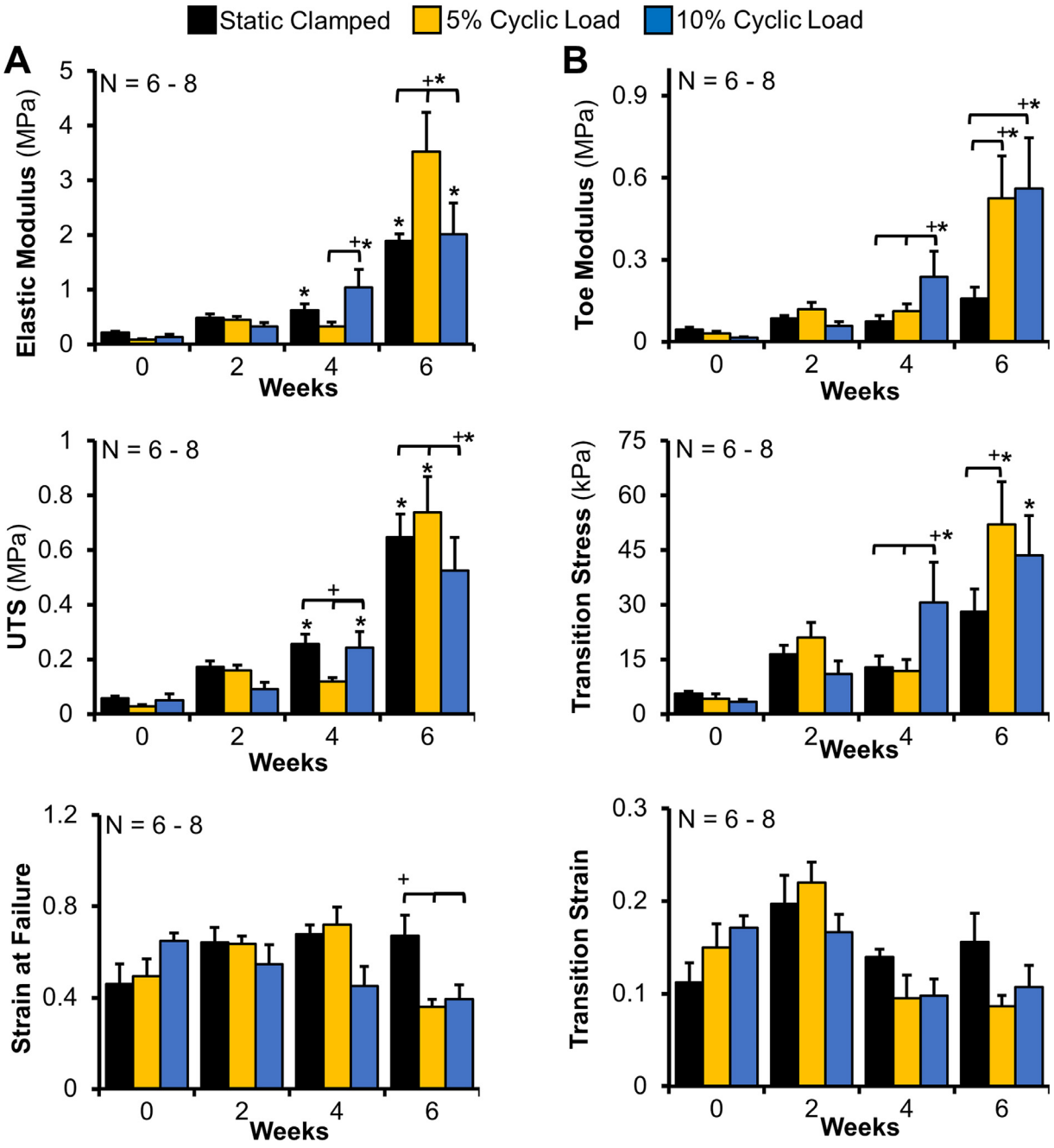

Fig. 5. Loading increased mechanical properties in a dose-dependent fashion. A) 5 % load constructs significantly improved elastic properties (Elastic modulus, ultimate tensile strength (UTS), and strain at failure) by 6 weeks compared to 10 % load and static samples. B) 5 % and 10 % load constructs significantly improved toe-region properties (Toe modulus, transition stress, and transition strain) by 6 weeks, suggesting increased fiber alignment and development of functional crimp. $N = 6–8$. Data shown as mean ± S.E.M., Significance compared to *0 week and +bracket group ($p < 0.05$).

of load drove increased collagen crimp formation and increased toe-region strength, suggesting the development of crimp is leading to more functional properties. By comparing to acellular gels, we demonstrated these improvements in collagen organization and tensile properties are cell driven, with the effect of cyclic load on cells varying depending on the degree of organization and magnitude of strain. Collectively, with respect to collagen production, cyclic load produced a more catabolic response early in culture while cells were in unorganized gels, and a more anabolic effect once cells were anchored on aligned fibrils, suggesting a shift in mechanotransduction with increased collagen organization. Further, while 10 % load drove further improvements in fiber organization, only 5 % cyclic strain produced increased elastic tensile properties and collagen accumulation, ultimately matching neonatal ACL properties, suggesting a mechanical threshold in cellular response.

Intermittent cyclic loading at or below 5 % strain is well established to improve fibril alignment, fibril diameter, and collagen production in engineered tendons and ligaments [1,5,20,27–37,62]; however the effect at the fiber and fascicle length-scale is largely unknown [1,25,29,39,63]. In this study we found that intermittent cyclic loading accelerates and improves hierarchical collagen organization at the fibril, fiber, and fascicle length-scale (Figs. 3 and 4). At the fibril level, similar to previous studies [62], 5 and 10 % cyclic

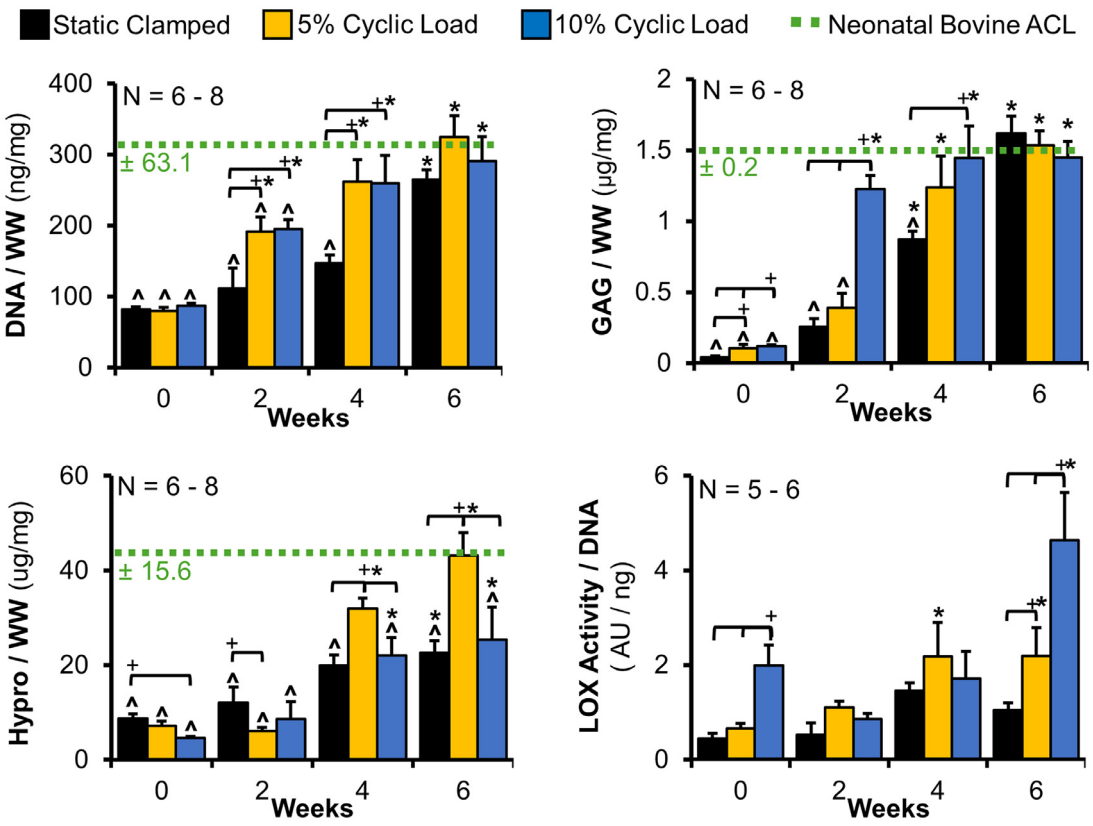

Fig. 6. Cells appeared to have a shift in mechanotransduction with time in culture, with 5 and 10 % load leading to differential changes in composition throughout culture. DNA, GAG, and collagen content, represented by hydroxyproline, normalized to wet weight (WW, $N = 6–8$), and LOX activity in constructs normalized to DNA ($N = 5–6$). 5 % load constructs matching neonatal ACL DNA, GAG, and collagen concentrations by 6 week. Data shown as mean ± S.E.M., Significance compared to *0 week, ^native, and +bracket group ($p < 0.05$).

load led to increased fibril alignment and fibril diameter, with both matching neonatal ACL alignment and 10 % load constructs developing fibril diameters that reach average native diameters by 6 weeks (Fig. 4B). Additionally, fibril diameters in both 5 % and 10 % load constructs became more heterogeneous by 6 weeks, similar to the shift observed in native fibril diameters during development [64]. Across species, ACL fibrils are reported to have an increase in diameter with age, with increasing distribution of diameters, ultimately resulting in a bimodal distribution of fibril diameters by maturity [65–72]. In particular, immature (4–5 month old) bovine ACL have been reported to have a spread of fibril diameters from 30 to 200 nm, without a bimodal distribution [67], similar to our neonatal bovine results. Thus, engineered constructs are following a similar path of development, and further maturation is needed to obtain larger fibrils, with a bimodal distribution and more pronounced fibril banding. At the fiber level, loading increased fiber alignment and diameter, with loaded constructs matching and exceeding neonatal ACL alignment by 2 weeks and fiber diameters by 4 weeks. At the fascicle length-scale, loaded constructs appeared to have improved early fascicle formation with qualitatively increased crimp formation by 6 weeks. Collectively, intermittent cyclic loading drove significant improvements at each hierarchical level over static controls, producing some of the largest and most hierarchically organized collagen fibers to date *in vitro*.

Further, we found that 10 % cyclic loading stimulated cells to produce larger and more organized hierarchical collagen fibers in comparison to 5 % load, with 10 % constructs having increased alignment and diameters at the fibril and fiber level (Figs. 3B & 4B). Traditionally strains at 5 % or below are reported to be optimal for tendon and ligament engineering [20,32–36], as most native tendons and ligaments experience strains under 5 % [73]. However, interestingly, here we found that 10 % cyclic strain led to improvements in fibril, fiber, and fascicle level organization compared to both static and 5 % load constructs. This may be due to the ACL receiving larger strain *in vivo* (up to 10–12 %) [40].

In addition to driving increased hierarchical organization, intermittent cyclic loading drove cells to produce collagen crimp starting at 2 weeks, with crimp appearing to increase in number and frequency by 6 weeks (Figs. 3 and 4). Crimps are wavy, planar zig zag structures in collagen fibers that serve a protective role in ligaments by taking on initial loads when strained [5,25,74,75]. Crimp formation is not well understood [7,76,77], but previous work has typically generated crimp structures by either manufacturing crimp into the scaffold prior to cell seeding [74,78–83], or by releasing restrained constructs post-seeding to allow for scaffold contraction [77]. Here, loading stimulated cellular development of crimp, evident by the fact that acellular constructs had no development of crimp even after 6 weeks of loading. *In vivo,* crimp develops postnatally as cells gather fibers into larger bundles [84]. Specifically, it has been reported crimp increases with increasing strain and maturation *in vivo* [76,77,85,86]. Similarly, in this study we observed increased crimp formation with applied dynamic cyclic strain and increasing hierarchical fiber maturation. It has been reported that collagen crimp in rat tail and Achilles tendons are fully extended at 4 % strain *in vivo* [75,87]. Previously, studies applying strains <5 % in scaffolds have not reported development of crimp [30,32,33], thus a strain greater than the natural crimp extension length of 4 % may be needed to stimulate cells to produce crimp. While both 5 % and 10 % load constructs appeared to formed crimp, 10 % load constructs appeared to form larger, more regularly spaced crimp. Ultimately, 10 % load constructs had crimp periods that were not significantly different from neonatal bovine,

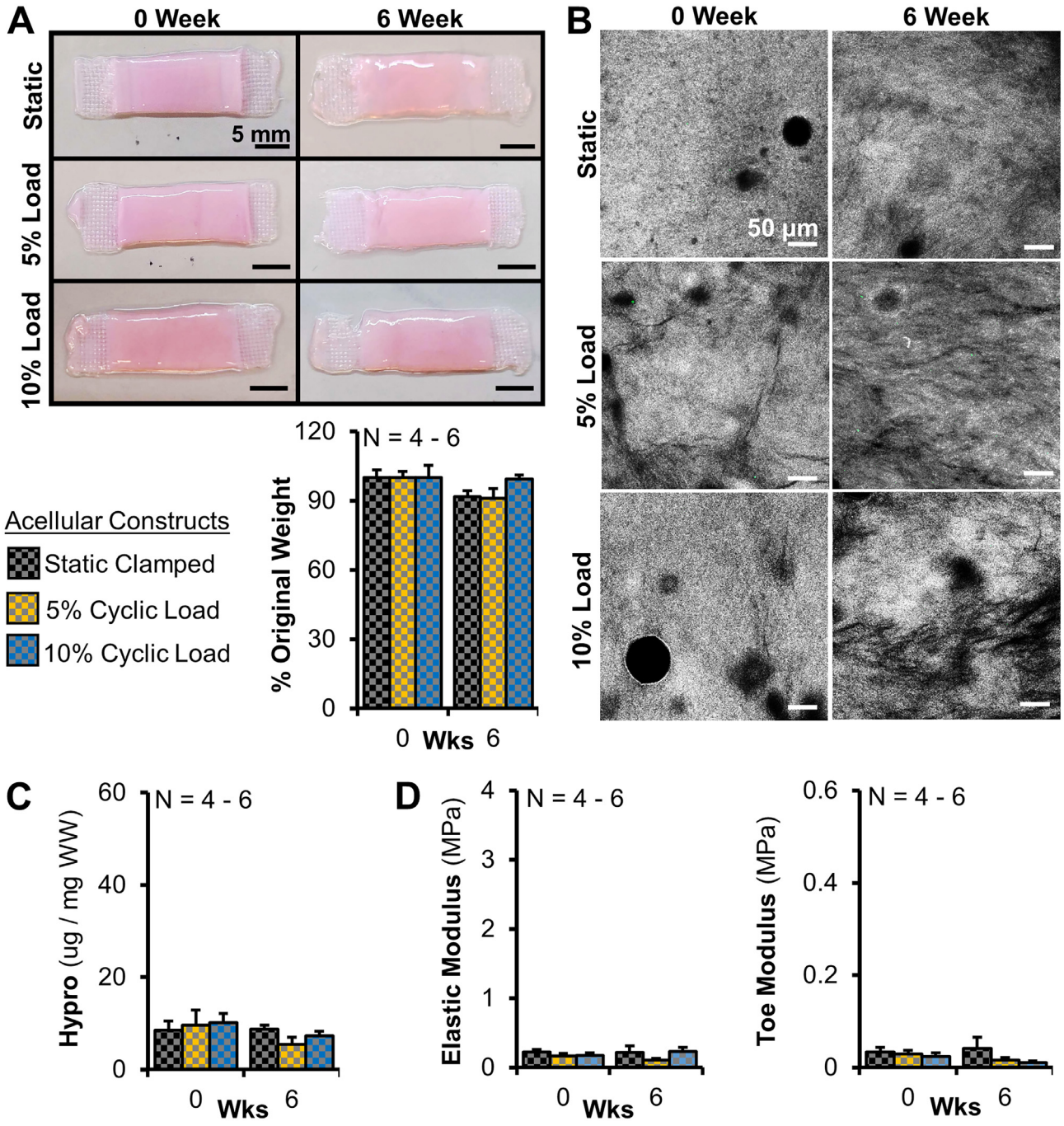

Fig. 7. Loading had little-to-no effect on acellular constructs, demonstrating changes in cell-seeded constructs in response to load are cell-driven. Acellular constructs had no significant change in A) gross morphology and percent weight by 6 weeks of culture. B) Confocal reflectance at 0 and 6 weeks revealed little-to-no change in organization (Grey = collagen, scale bar = 50 μm). C) Collagen content, represented by hydroxyproline and normalized to wet weight (WW), and D) Tensile properties (elastic and toe modulus) had no increases with time in culture (y-axis set to similar scale used for cell-seeded constructs, see Supplemental Figure 3 for y-axis fit to acellular data). Data shown as mean ± S.E.M., Significance compared to *0 week and +bracket group ($p < 0.05$).

and reached crimp lengths previously reported for mature human and ovine ACLs [55–58]. This suggests that there may be a dose-dependent response to load in the formation of crimp. Crimp is important to proper ligament function, however it is still unknown how it is formed. Our system could be a promising means to further explore what regulates cellular production of crimp.

As mentioned previously, crimp serves a protective role in ligaments by taking on initial loads when strains are applied [5,75,88], thus collagen crimp contributes largely to the toe region of the stress-strain curve. Here, toe region properties improved 2.5–3.5 fold for loaded constructs over static controls (Fig. 5B), suggesting the development of crimp may be playing a functional role [13]. When comparing mature collagen fibers with and without crimp, it would be expected that the presence of crimp would decrease toe modulus and increased transition strain, which we did not find. However, our engineered tissues are maturing as developing crimp, which makes it difficult to distinguish the effect of crimp from others changes in the tissue such as increased fibril alignment, diameter, or crosslinking. Interestingly, similar results have been found in the developing mouse Achilles tendon, where transition stress and toe modulus were found to increases from postnatal day 4 to 28, while transition strain decreased [65]. Further, crimp is reported

to start developing in mouse tendons as early as 14 days, demonstrating toe region properties do increase as crimp and collagen fibers develop [89,90], similar to our engineered constructs. Unfortunately, we were unable to mechanical test immature bovine ACL for full comparison of toe region data, however, increases in tensile strength and stiffness, as well as decreases in strain properties (transition, yield, and ultimate strain) are needed to better match mature human ACL (elastic moduli ~100–200 MPa and failure strains ~0.3–0.5 [91,92]), demonstrating the need for further maturation. Another limitation to this study is preconditioning was not performed prior to mechanical tests which could affected the reported toe region properties. Tests without preconditioning are common in engineered tissues since preconditioning can induce fibril organization which can bias mechanical data [25,26,43,45,53]. However, future studies should use preconditioning for a better understanding of toe region properties.

Interestingly, despite both 5 and 10 % load producing increased toe region properties and increased hierarchical organization, only 5 % load produced a significant increase in elastic region tensile properties over static controls (Fig. 5A). As hierarchical collagen organization increases throughout development so too does tensile strength [14,93,94]. Similarly, in this study, as hierarchical organization improved in all constructs with time in culture, so too did tensile strength. By 6 weeks, the elastic modulus of all groups reached the reported range of immature 1 week old bovine ACL (1–3 MPa) [61], however 5 % load constructs exceeded this range (Fig. 5A) despite being less organized than 10 % load constructs. The size and organization of collagen fibers is not the sole determining factor for tissue tensile strength. It has been reported that tissue strength is reliant on collagen fiber orientation, density, diameter, and degree of crosslinking [6,95–98]. Cyclic loading, particularly 5 % load significantly increased collagen content by 6 weeks of culture, with 5 % load constructs reaching neonatal bovine ACL collagen concentrations (Fig 6). This increase in collagen content in 5 % load constructs may explain the improved elastic modulus. However, while 10 % load did not increase collagen accumulation over static controls, it did stimulate increased LOX activity at 0 and 6 weeks.

LOX is an enzyme produced by cells which naturally crosslinks collagen. LOX crosslinks are another critical element in providing mechanical strength and transferring load between fibrils [5,6,95–98]. It is not well understood how mature LOX crosslinks form [99,100], but it is thought to be due to a cellular response to load [96,101,102]. In this study loading significantly increased LOX activity temporally throughout culture, with 10 % load inducing a 2-fold higher activity at 0 and 6 weeks in comparison to 5 % load (Fig. 6). It has been previously reported that cyclic loading of mature tendons stimulates or activates the cellular mechanical stretch ion channel PIEZO1 and it has been suggested this activation of PIEZO1 stimulates LOX synthesis, producing stronger tendons [102]. Further, it has been reported PIEZO1 is strain dependent in chondrocytes, with only strains higher than 8 % triggering the channel [101,103–105]. While strain dependency of PIEZO1 has not been studied in the ACL, these ion channels are likely also strain-dependent in ligament fibroblasts. Thus, this may explain why 10 % cyclic load resulted in a 2-fold increase in LOX activity over 5 % load.

Surprisingly, even though LOX activity was increased with 10 % cyclic loading, there was no corresponding increase in tensile strength. This lack of increase in tensile strength may be because LOX initially forms immature divalent crosslinks which do not have a significant effect on tissue strength [106,107]. With time these crosslinks can condense into mature trivalent crosslinks, which are believed to be a primary source of strength in collagen fibers [98,100,108,109]. These mature trivalent crosslinks take weeks-to-months to form *in vivo* and *in vitro* [43,99,100,107]. Therefore, the 10 % load constructs may need more time in culture to form trivalent crosslinks, which may then increase tissue tensile strength. One limitation of this study was we did not measure LOX crosslinks directly. Future studies should evaluate divalent, trivalent, and longer culture durations to evaluate whether increases in LOX activity led to improved functional biochemical and mechanical properties.

Interestingly, 10 % cyclic loading only significantly increased LOX activity at 0 and 6 weeks (Fig 6). This temporal LOX activity reflects a previous study from our lab which found a similar release pattern of LOX activity in the media of static clamped constructs [43], and this pattern closely mirrors previously reported results in developing chick calcaneal tendons, where LOX activity increased temporally throughout development, with more dramatic increases at later stages of development [108,109]. Another explanation for this temporal LOX activity may be a change in mechanotransduction with time in culture. We hypothesize that as our constructs mature from unorganized collagen to aligned fibrils, the cells within our constructs experience the loads differently and receive higher loads [110], ultimately altering their response to the load.

In addition to differences in LOX activity with time in culture, cells differentially regulated collagen, DNA, and GAG. In this study, cells differentially regulated collagen production depending on degree of organization and magnitude of load, with cyclic load first producing a catabolic response early in culture when cells were in unorganized gels, which later shifted to an anabolic response once cells were anchored on aligned fibrils and fibers (Fig. 6). We have previously found in our system that the most collagen turnover occurs in the first 2 weeks as cells produce aligned fibrils [25,45,53]. Here, we found similar results, with loading increasing collagen turnover in the first 2 weeks resulting in reduced collagen concentrations at 2 weeks. However, once aligned fibrils were formed at 2 weeks, loading significantly increased collagen accumulation with 5 % load constructs accumulating significantly more collagen than 10 % load and static constructs. Previous work has reported cells produce more collagen on aligned surfaces [30], in the presence of crimp [13], and with mechanical load [13], which we also found to be the case with our cultures. Further, it has been reported that cells sense load more intensely when attached to aligned fibers, which may lead to shifts in mechanotransduction [110]. Therefore, as cells produce aligned fibrils and fibers in our system, they may be sensing more load, which in the case of 5 % cyclic load results in increased collagen production and in the case of 10 % load produced larger fibril and fiber diameters. However, there may be a threshold in cellular response. Higher loads may lead to a reduced anabolic response or a higher catabolic response [29,74], possibly accounting for the limited increase in collagen concentration for 10 % load constructs later in culture. Further, while cellular responses appear to correlate with changes in organization, they could be due to other changes, such as changes in mechanical properties or time in culture, thus a better evaluation of these differences as well as local response of cells across the construct with changes in organization are interesting points for future studies.

Further, loading differentially stimulated DNA and GAG accumulation throughout culture as well, but in an opposite manner as collagen accumulation. Intermittent cyclic loading increased DNA and GAG accumulation early in culture while cells were in unorganized collagen, but leveled off at native DNA and GAG concentration later in culture once cells were anchored on aligned fibrils and fibers, further suggesting a change in mechanotransduction. Cyclic stimulation is reported to increase cell proliferation in a dose-dependent manner with higher strains producing increased proliferation [111,112]. Here we found cyclic loading increased DNA concentrations in the first 4 weeks, suggesting increased proliferation, however we did not find a difference between 5 and 10 %

load (Fig. 6). In contrast, we did find a dose-dependent response with GAG accumulation, with 10 % load significantly increasing GAG at 2 and 4 weeks over 5 % and static constructs. Typically, levels above 5 % strain are not used for tendon and ligament engineering because they are thought to be pathological, one sign of which is increased GAGs [113,114]. In particular, GAGs such as aggrecan and larger proteoglycans are not generally found in ligaments unless overloaded [113,114]. However, in this study, even though 10 % loading produced increases in GAGs early in culture, these constructs leveled off once reaching native GAG levels, reducing the likelihood that loading induced a pathological response. Instead, this may suggest higher magnitude cyclic strains have a great effect on cell production of small leucine rich proteoglycans (SLRPs), a subset of GAGs, which have been shown to play a role in controlling fiber size and organization, and are established to increase with development and maturation [13,115]. Future studies should evaluate the type of GAGs and collagen produced to gain a better understanding of cellular regulation of SLRPs and hierarchical collagen fiber formation.

Here, we significantly accelerated and increased hierarchical collagen fiber formation, induced early crimp formation, and increased tissue tensile strength to match or exceed that of immature ACL. Further, we have developed a system which provides an opportunity to explore how cellular mechanotransduction changes with increasing hierarchical collagen organization. However, this work is not without limitations. While these are some of the most organized ligament replacements to date, further maturation is needed to reach mature organization, composition, and tensile strength. This study was an initial foray in evaluating the effect of cyclic load on cell driven hierarchical organization and thus, we focused on the high and low ends of the spectrum of strain measured in native ACL (up to 5–12 %) [40]. Potentially, higher strains, longer cultures, or a combination of different loading cues are needed for further maturation. Further, the intermittent loading regime used in this study (1 Hz, 1 hour on, 1 hour off, 1 hour on, 3x per week) is specifically tailored for optimal matrix turnover in unorganized gels resulting in increased matrix accumulation [42,45–48], but changing any aspect such as magnitude, frequency, duration, or rest period at any point in culture could change outcomes. In particular, here we found cellular response to load varied with organization, with 10 % cyclic load improving properties early in culture when cells are in unorganized gels, and 5 % load driving improvements later in culture, once cells are anchored on aligned fibrils. This suggests that a load control regime or adaptive loading regimes which changes magnitude, duration, or frequency as the tissue develops may be needed to drive further maturation. However, despite these limitations, this study provides new insight into how intermittent cyclic loading affects cell-driven hierarchical fiber formation and how cells respond to these loads differentially depending on degree of maturation. A better understanding of how mechanical cues regulate fiber formation beyond the fibril level will help to develop better rehabilitation protocols to drive repair *in vivo* and improve loading protocols to drive collagen fiber maturation in engineered tissues.

5. Conclusions

Collectively, this study demonstrates intermittent cyclic loading at strains that reflect the native ACL environment accelerate and improve hierarchical collagen organization, crimp formation, and tissue tensile strength, producing constructs that match or exceed the properties of immature ACL. Further, we demonstrated these improvements in collagen organization and mechanical properties were cell driven, with the effect of cyclic load on cells varying depending on the degree of organization and magnitude of strain. We found 10 % cyclic load drove early improvements in tensile properties and composition when cells were in unorganized gels, while 5 % load was more beneficial later in culture once cells were anchored on aligned fibers, suggesting a shift in mechanotransduction or a cellular threshold to response. Currently, it is not well understood how cells regulate hierarchical collagen fiber formation and little is known about cellular response to load beyond the fibril level [1,14,41]. This study provides new insight into how cyclic loading affects cell-driven hierarchical fiber formation. A better understanding of how mechanical cues regulate fiber formation will help to better engineer replacements and develop better rehabilitation protocols to drive repair after injury.

Declaration of competing interest

The authors declare that they have no known competing financial interests or personal relationships that could have appeared to influence the work reported in this paper.

CRediT authorship contribution statement

Leia D. Troop: Writing – review & editing, Writing – original draft, Methodology, Investigation, Formal analysis, Data curation, Conceptualization. **Jennifer L. Puetzer:** Writing – review & editing, Writing – original draft, Supervision, Resources, Project administration, Funding acquisition, Formal analysis, Data curation, Conceptualization.

Acknowledgements

The authors would like to thank Drs. Carl Mayer, Dmitry Pestov, and Ethan Brown for their assistance with this study. The authors acknowledge the use of facilities within the Nanomaterials Characterization Core and the Virginia Commonwealth University Cancer Mouse Models Core Laboratory, supported in part, with funding from NIH–NCI Cancer Center Support Grant P30 CA016059.

Funding Information

This work was supported, in part, by a pilot Interdisciplinary Rehabilitation Engineering Research Career Development grant supported by the Eunice Kennedy Shiver National Institute of Child Health and Human Development of the National Institutes of Health (Award Number K12HD073945), a NSF CAREER award (CCMI 2045995), and a National Science Foundation Graduate Research Fellowship (Grant No. 1650114).

Supplementary materials

Supplementary material associated with this article can be found, in the online version, at doi:10.1016/j.actbio.2024.07.025.

References

[1] M.T. Galloway, A.L. Lalley, J.T. Shearn, The role of mechanical loading in tendon development, maintenance, injury, and repair, J. Bone Joint Surg. Am. 95 (2013) 1620–1628, doi:10.2106/JBJS.L.01004.
[2] K.E. Glattke, S.V. Tummala, A. Chhabra, Anterior cruciate ligament reconstruction recovery and rehabilitation: a systematic review, JBJS 104 (2022) 739, doi:10.2106/JBJS.21.00688.
[3] K.L. Goh, A. Listrat, D. Béchet, Hierarchical mechanics of connective tissues: integrating insights from nano to macroscopic studies, J. Biomed. Nanotechnol. 10 (2014) 2464–2507, doi:10.1166/jbn.2014.1960.
[4] G. Yang, B.B. Rothrauff, R.S. Tuan, Tendon and ligament regeneration and repair: clinical relevance and developmental paradigm, Birth Defects Res. Part C 99 (2013) 203–222, doi:10.1002/bdrc.21041.
[5] B.K. Connizzo, S.M. Yannascoli, L.J. Soslowsky, Structure-function relationships of postnatal tendon development: a parallel to healing, Matrix Biol. J. Int. Soc. Matrix Biol. 32 (2013) 106–116, doi:10.1016/j.matbio.2013.01.007.
[6] M.J. Buehler, Nature designs tough collagen: explaining the nanostructure of collagen fibrils, Proc. Natl. Acad. Sci. 103 (2006) 12285–12290, doi:10.1073/pnas.0603216103.

[7] G. Zhang, B.B. Young, Y. Ezura, M. Favata, L.J. Soslowsky, S. Chakravarti, D.E. Birk, Development of tendon structure and function: regulation of collagen fibrillogenesis, J. Musculoskelet. Neuronal Interact. 5 (2005) 5–21.
[8] N. Karathanasopoulos, J. Ganghoffer, Investigating the effect of aging on the viscosity of tendon fascicles and fibers, Front. Bioeng. Biotechnol. 7 (2019), doi:10.3389/fbioe.2019.00107.
[9] M. Pierantoni, I. Silva Barreto, M. Hammerman, V. Novak, A. Diaz, J. Engqvist, P. Eliasson, H. Isaksson, Multimodal and multiscale characterization reveals how tendon structure and mechanical response are altered by reduced loading, Acta Biomater. 168 (2023) 264–276, doi:10.1016/j.actbio.2023.07.021.
[10] N. Karathanasopoulos, P. Angelikopoulos, C. Papadimitriou, P. Koumoutsakos, Bayesian identification of the tendon fascicle's structural composition using finite element models for helical geometries, Comput. Methods Appl. Mech. Eng. 313 (2017) 744–758, doi:10.1016/j.cma.2016.10.024.
[11] R.B. Svensson, P. Hansen, T. Hassenkam, B.T. Haraldsson, P. Aagaard, V. Kovanen, M. Krogsgaard, M. Kjaer, S.P. Magnusson, Mechanical properties of human patellar tendon at the hierarchical levels of tendon and fibril, J. Appl. Physiol. 112 (2012) 419–426, doi:10.1152/japplphysiol.01172.2011.
[12] A. Gautieri, S. Vesentini, A. Redaelli, M.J. Buehler, Hierarchical structure and nanomechanics of collagen microfibrils from the atomistic scale up, Nano Lett 11 (2011) 757–766, doi:10.1021/nl103943u.
[13] Z. Chen, B. Zhou, X. Wang, G. Zhou, W. Zhang, B. Yi, W. Wang, W. Liu, Synergistic effects of mechanical stimulation and crimped topography to stimulate natural collagen development for tendon engineering, Acta Biomater. 145 (2022) 297–315, doi:10.1016/j.actbio.2022.04.026.
[14] T. Nau, A. Teuschl, Regeneration of the anterior cruciate ligament: current strategies in tissue engineering, World J. Orthop. 6 (2015) 127–136, doi:10.5312/wjo.v6.i1.127.
[15] M.T. Rodrigues, R.L. Reis, M.E. Gomes, Engineering tendon and ligament tissues: present developments towards successful clinical products, J. Tissue Eng. Regen. Med. 7 (2013) 673–686, doi:10.1002/term.1459.
[16] E. Hing, D.K. Cherry, D.A. Woodwell, National Ambulatory Medical Care Survey: 2004 summary, Adv. Data (2006) 1–33.
[17] J. Wong, V. Barrass, N. Maffulli, Quantitative review of operative and nonoperative management of achilles tendon ruptures, Am. J. Sports Med. 30 (2002) 565–575, doi:10.1177/03635465020300041701.
[18] D. Sugimoto, J.C. LeBlanc, S.E. Wooley, L.J. Micheli, D.E. Kramer, The effectiveness of a functional knee brace on joint-position sense in anterior cruciate ligament–reconstructed individuals, J. Sport Rehabil. 25 (2016) 190–194, doi:10.1123/jsr.2014-0226.
[19] S. Patel, J.-M. Caldwell, S.B. Doty, W.N. Levine, S. Rodeo, L.J. Soslowsky, S. Thomopoulos, H.H. Lu, Integrating soft and hard tissues via interface tissue engineering, J. Orthop. Res. 36 (2018) 1069–1077, doi:10.1002/jor.23810.
[20] M.T.K. Bramson, S.K. Van Houten, D.T. Corr, Mechanobiology in tendon, ligament, and skeletal muscle tissue engineering, J. Biomech. Eng. (2021) 143, doi:10.1115/1.4050035.
[21] M.V. Paterno, S. Thomas, K.T. VanEtten, L.C. Schmitt, Confidence, ability to meet return to sport criteria, and second ACL injury risk associations after ACL-reconstruction, J. Orthop. Res. 40 (2022) 182–190, doi:10.1002/jor.25071.
[22] V. Kandhari, T.D. Vieira, H. Ouanezar, C. Praz, N. Rosenstiel, C. Pioger, F. Franck, A. Saithna, B. Sonnery-Cottet, Clinical outcomes of arthroscopic primary anterior cruciate ligament repair: a systematic review from the scientific anterior cruciate ligament network international study group, Arthroscopy 36 (2020) 594–612, doi:10.1016/j.arthro.2019.09.021.
[23] M.M. Murray, B.C. Fleming, G.J. Badger, C. Freiberger, R. Henderson, S. Barnett, A. Kiapour, K. Ecklund, B. Proffen, N. Sant, D.E. Kramer, L.J. Micheli, Y.-M. Yen, Bridge-enhanced anterior cruciate ligament repair is not inferior to autograft anterior cruciate ligament reconstruction at 2 years: results of a prospective randomized clinical trial, Am. J. Sports Med. 48 (2020) 1305–1315, doi:10.1177/0363546520913532.
[24] A.U. Khan, R. Aziz, M. Reen, W. Walker, P. Myers, The first case of bridge-enhanced Anterior Cruciate Ligament (ACL) repair (BEAR) procedure in Mississippi, Cureus (2023), doi:10.7759/cureus.44218.
[25] J.L. Puetzer, T. Ma, I. Sallent, A. Gelmi, M.M. Stevens, Driving hierarchical collagen fiber formation for functional tendon, ligament, and meniscus replacement, Biomaterials 269 (2021) 120527, doi:10.1016/j.biomaterials.2020.120527.
[26] M.E. Brown, J.L. Puetzer, Driving native-like zonal enthesis formation in engineered ligaments using mechanical boundary conditions and β-tricalcium phosphate, Acta Biomater. 140 (2022) 700–716, doi:10.1016/j.actbio.2021.12.020.
[27] W. Shen, X. Chen, Y. Hu, Z. Yin, T. Zhu, J. Hu, J. Chen, Z. Zheng, W. Zhang, J. Ran, B.C. Heng, J. Ji, W. Chen, H.-W. Ouyang, Long-term effects of knitted silk–collagen sponge scaffold on anterior cruciate ligament reconstruction and osteoarthritis prevention, Biomaterials 35 (2014) 8154–8163, doi:10.1016/j.biomaterials.2014.06.019.
[28] J. Ma, M.J. Smietana, T.Y. Kostrominova, E.M. Wojtys, L.M. Larkin, E.M. Arruda, Three-dimensional engineered bone–ligament–bone constructs for anterior cruciate ligament replacement, Tissue Eng. Part A 18 (2012) 103–116, doi:10.1089/ten.tea.2011.0231.
[29] L. Paschall, S. Carrozzi, E. Tabdanov, A. Dhawan, S.E. Szczesny, Cyclic loading induces anabolic gene expression in ACLs in a load-dependent and sex-specific manner, J. Orthop. Res. 42 (2023) 267–276, doi:10.1002/jor.25677.
[30] B.M. Baker, R.P. Shah, A.H. Huang, R.L. Mauck, Dynamic tensile loading improves the functional properties of mesenchymal stem cell-laden nanofiber-based fibrocartilage, Tissue Eng. Part A 17 (2011) 1445–1455, doi:10.1089/ten.tea.2010.0535.
[31] W.K. Grier, R.A. Sun Han Chang, M.D. Ramsey, B.A.C. Harley, The influence of cyclic tensile strain on multi-compartment collagen-GAG scaffolds for tendon-bone junction repair, Connect. Tissue Res. 60 (2019) 530–543, doi:10.1080/03008207.2019.1601183.
[32] K. Mubyana, D.T. Corr, Cyclic Uniaxial Tensile Strain Enhances the Mechanical Properties of Engineered, Scaffold-Free Tendon Fibers, Tissue Eng. Part A 24 (2018) 1808–1817, doi:10.1089/ten.tea.2018.0028.
[33] N.R. Schiele, R.A. Koppes, D.B. Chrisey, D.T. Corr, Engineering cellular fibers for musculoskeletal soft tissues using directed self-assembly, Tissue Eng. Part A 19 (2013) 1223–1232, doi:10.1089/ten.tea.2012.0321.
[34] E. Maeda, J.C. Shelton, D.L. Bader, D.A. Lee, Time dependence of cyclic tensile strain on collagen production in tendon fascicles, Biochem. Biophys. Res. Commun. 362 (2007) 399–404, doi:10.1016/j.bbrc.2007.08.029.
[35] R.J. Crockett, M. Centrella, T.L. McCarthy, J.G. Thomson, Effects of cyclic strain on rat tail tenocytes, Mol. Biol. Rep. 37 (2010) 2629–2634, doi:10.1007/s11033-009-9788-8.
[36] J.A. Hannafin, S.P. Arnoczky, A. Hoonjan, P.A. Torzilli, Effect of stress deprivation and cyclic tensile loading on the material and morphologic properties of canine flexor digitorum profundus tendon: an *in vitro* study, J. Orthop. Res. 13 (1995) 907–914, doi:10.1002/jor.1100130615.
[37] J.L. Puetzer, L.J. Bonassar, High density type I collagen gels for tissue engineering of whole menisci, Acta Biomater. 9 (2013) 7787–7795, doi:10.1016/j.actbio.2013.05.002.
[38] S.E. Szczesny, D.T. Corr, Tendon cell and tissue culture: perspectives and recommendations, J. Orthop. Res. 41 (2023) 2093–2104, doi:10.1002/jor.25532.
[39] N.A. Dyment, J.G. Barrett, H.A. Awad, C.A. Bautista, A.J. Banes, D.L. Butler, A brief history of tendon and ligament bioreactors: impact and future prospects, J. Orthop. Res. 38 (2020) 2318–2330, doi:10.1002/jor.24784.
[40] Z.A. Englander, W.E. Garrett, C.E. Spritzer, L.E. DeFrate, *In vivo* attachment site to attachment site length and strain of the ACL and its bundles during the full gait cycle measured by MRI and high-speed biplanar radiography, J. Biomech. 98 (2020) 109443, doi:10.1016/j.jbiomech.2019.109443.
[41] T. Wang, P. Chen, M. Zheng, A. Wang, D. Lloyd, T. Leys, Q. Zheng, M.H. Zheng, *In vitro* loading models for tendon mechanobiology, J. Orthop. Res. 36 (2018) 566–575, doi:10.1002/jor.23752.
[42] M.E. Brown, J.L. Puetzer, Enthesis maturation in engineered ligaments is differentially driven by loads that mimic slow growth elongation and rapid cyclic muscle movement, Acta Biomater. 172 (2023) 106–122, doi:10.1016/j.actbio.2023.10.012.
[43] M.E. Bates, L. Troop, M.E. Brown, J.L. Puetzer, Temporal application of lysyl oxidase during hierarchical collagen fiber formation differentially effects tissue mechanics, Acta Biomater. 160 (2023) 98–111, doi:10.1016/j.actbio.2023.02.024.
[44] V.L. Cross, Y. Zheng, N. Won Choi, S.S. Verbridge, B.A. Sutermaster, L.J. Bonassar, C. Fischbach, A.D. Stroock, Dense type I collagen matrices that support cellular remodeling and microfabrication for studies of tumor angiogenesis and vasculogenesis *in vitro*, Biomaterials 31 (2010) 8596–8607, doi:10.1016/j.biomaterials.2010.07.072.
[45] J.L. Puetzer, L.J. Bonassar, Physiologically distributed loading patterns drive the formation of zonally organized collagen structures in tissue-engineered meniscus, Tissue Eng. Part A 22 (2016) 907–916, doi:10.1089/ten.tea.2015.0519.
[46] J.J. Ballyns, L.J. Bonassar, Dynamic compressive loading of image-guided tissue engineered meniscal constructs, J. Biomech. 44 (2011) 509–516, doi:10.1016/j.jbiomech.2010.09.017.
[47] G.D. Nicodemus, S.J. Bryant, Mechanical loading regimes affect the anabolic and catabolic activities by chondrocytes encapsulated in PEG hydrogels, Osteoarthritis Cartilage 18 (2010) 126–137, doi:10.1016/j.joca.2009.08.005.
[48] J.D. Kisiday, J.H. Lee, P.N. Siparsky, D.D. Frisbie, C.R. Flannery, J.D. Sandy, A.J. Grodzinsky, Catabolic responses of chondrocyte-seeded peptide hydrogel to dynamic compression, Ann. Biomed. Eng. 37 (2009) 1368–1375, doi:10.1007/s10439-009-9699-9.
[49] J.L. Puetzer, J.J. Ballyns, L.J. Bonassar, The effect of the duration of mechanical stimulation and post-stimulation culture on the structure and properties of dynamically compressed tissue-engineered menisci, Tissue Eng. Part A 18 (2012) 1365–1375, doi:10.1089/ten.tea.2011.0589.
[50] B.D. Beynnon, B.C. Fleming, Anterior cruciate ligament strain in-vivo: a review of previous work, J. Biomech. 31 (1998) 519–525, doi:10.1016/S0021-9290(98)00044-X.
[51] J. Ma, H. Narayanan, K. Garikipati, K. Grosh, E.M. Arruda, Experimental and computational investigation of viscoelasticity of native and engineered ligament and tendon, in: K. Garikipati, E.M. Arruda (Eds.), IUTAM Symp. Cell. Mol. Tissue Mech., Springer Netherlands, Dordrecht, 2010, pp. 3–17, doi:10.1007/978-90-481-3348-2_1.
[52] Y. Kimura, A. Hokugo, T. Takamoto, Y. Tabata, H. Kurosawa, Regeneration of anterior cruciate ligament by biodegradable scaffold combined with local controlled release of basic fibroblast growth factor and collagen wrapping, Tissue Eng. Part C 14 (2008) 47–57, doi:10.1089/tec.2007.0286.
[53] J.L. Puetzer, E. Koo, L.J. Bonassar, Induction of fiber alignment and mechanical anisotropy in tissue engineered menisci with mechanical anchoring, J. Biomech. 48 (2015) 1436–1443, doi:10.1016/j.jbiomech.2015.02.033.
[54] I.F. Williams, A.S. Craig, D.A.D. Parry, A.E. Goodship, J. Shah, I.A. Silver, Development of collagen fibril organization and collagen crimp patterns dur-

ing tendon healing, Int. J. Biol. Macromol. 7 (1985) 275–282, doi:10.1016/0141-8130(85)90025-X.
[55] A. Weiler, F.N. Unterhauser, H.-J. Bail, M. Hüning, N.P. Haas, α-Smooth muscle actin is expressed by fibroblastic cells of the ovine anterior cruciate ligament and its free tendon graft during remodeling, J. Orthop. Res. 20 (2002) 310–317, doi:10.1016/S0736-0266(01)00109-7.
[56] A. Weiler, C. Förster, P. Hunt, R. Falk, T. Jung, F.N. Unterhauser, V. Bergmann, G. Schmidmaier, N.P. Haas, The influence of locally applied platelet-derived growth factor-BB on free tendon graft remodeling after anterior cruciate ligament reconstruction, Am. J. Sports Med. 32 (2004) 881–891, doi:10.1177/0363546503261711.
[57] M. Weiss, F.N. Unterhauser, A. Weiler, Crimp frequency is strongly correlated to myofibroblast density in the human anterior cruciate ligament and its autologous tendon grafts, Knee Surg. Sports Traumatol. Arthrosc. 20 (2012) 889–895, doi:10.1007/s00167-011-1644-4.
[58] L. Zhao, A. Thambyah, N. Broom, Crimp morphology in the ovine anterior cruciate ligament, J. Anat. 226 (2015) 278–288, doi:10.1111/joa.12276.
[59] B.O. Enobakhare, D.L. Bader, D.A. Lee, Quantification of sulfated glycosaminoglycans in chondrocyte/alginate cultures, by use of 1,9-dimethylmethylene blue, Anal. Biochem. 243 (1996) 189–191, doi:10.1006/abio.1996.0502.
[60] G. Kesava Reddy, C.S. Enwemeka, A simplified method for the analysis of hydroxyproline in biological tissues, Clin. Biochem. 29 (1996) 225–229, doi:10.1016/0009-9120(96)00003-6.
[61] S.V. Eleswarapu, D.J. Responte, K.A. Athanasiou, Tensile properties, collagen content, and crosslinks in connective tissues of the immature knee joint, PLoS ONE 6 (2011) e26178, doi:10.1371/journal.pone.0026178.
[62] A.J. Janvier, E.G. Pendleton, L.J. Mortensen, D.C. Green, J.R. Henstock, E.G. Canty-Laird, Multimodal analysis of the differential effects of cyclic strain on collagen isoform composition, fibril architecture and biomechanics of tissue engineered tendon, J. Tissue Eng. 13 (2022) 20417314221130486, doi:10.1177/20417314221130486.
[63] Y. Xu, Q. Wang, Y. Li, Y. Gan, P. Li, S. Li, Y. Zhou, Q. Zhou, Cyclic tensile strain induces tenogenic differentiation of tendon-derived stem cells in bioreactor culture, BioMed Res. Int. 2015 (2015) e790804, doi:10.1155/2015/790804.
[64] K.E. Kadler, D.F. Holmes, J.A. Trotter, J.A. Chapman, Collagen fibril formation, Biochem. J. 316 (1996) 1–11, doi:10.1042/bj3160001.
[65] H.L. Ansorge, S. Adams, D.E. Birk, L.J. Soslowsky, Mechanical, compositional, and structural properties of the post-natal mouse achilles tendon, Ann. Biomed. Eng. 39 (2011) 1904–1913, doi:10.1007/s10439-011-0299-0.
[66] Z. Beisbayeva, A. Zhanbassynova, G. Kulzhanova, F. Mukasheva, C. Erisken, Change in collagen fibril diameter distribution of bovine anterior cruciate ligament upon injury can be mimicked in a nanostructured scaffold, Molecules 26 (2021) 1204, doi:10.3390/molecules26051204.
[67] D. Qu, P.J. Chuang, S. Prateepchinda, P.S. Balasubramanian, X. Yao, S.B. Doty, C.P. Hendon, H.H. Lu, Micro- and ultrastructural characterization of age-related changes at the anterior cruciate ligament-to-bone insertion, ACS Biomater. Sci. Eng. 3 (2017) 2806–2814, doi:10.1021/acsbiomaterials.6b00602.
[68] S. Smatov, F. Mukasheva, C. Erisken, Collagen fibril diameter distribution of sheep anterior cruciate ligament, Polymers 15 (2023) 752, doi:10.3390/polym15030752.
[69] S. Kadyr, U. Nurmanova, B. Khumyrzakh, A. Zhakypbekova, D. Saginova, N. Daniyeva, C. Erisken, Braided biomimetic PCL grafts for anterior cruciate ligament repair and regeneration, Biomed. Mater. Bristol Engl. 19 (2024), doi:10.1088/1748-605X/ad2555.
[70] A. Oryan, A.H. Shoushtari, Histology and ultrastructure of the developing superficial digital flexor tendon in rabbits, Anat. Histol. Embryol. 37 (2008) 134–140, doi:10.1111/j.1439-0264.2007.00811.x.
[71] D.a.D. Parry, A.S. Craig, G.R.G. Barnes, D.C. Phillips, Tendon and ligament from the horse: an ultrastructural study of collagen fibrils and elastic fibres as a function of age, Proc. R. Soc. Lond. B 203 (1997) 293–303, doi:10.1098/rspb.1978.0106.
[72] D.A.D. Parry, G.R.G. Barnes, A.S. Craig, A comparison of the size distribution of collagen fibrils in connective tissues as a function of age and a possible relation between fibril size distribution and mechanical properties, Proc. R. Soc. Lond. B (1978), doi:10.1098/rspb.1978.0107.
[73] H. Delport, L. Labey, R. De Corte, B. Innocenti, J. Vander Sloten, J. Bellemans, Collateral ligament strains during knee joint laxity evaluation before and after TKA, Clin. Biomech. 28 (2013) 777–782, doi:10.1016/j.clinbiomech.2013.06.006.
[74] Y.J. No, M. Castilho, Y. Ramaswamy, H. Zreiqat, Role of biomaterials and controlled architecture on tendon/ligament repair and regeneration, Adv. Mater. 32 (2020) 1904511, doi:10.1002/adma.201904511.
[75] M. Franchi, A. Trirè, M. Quaranta, E. Orsini, V. Ottani, Collagen structure of tendon relates to function, Sci. World J. 7 (2007) 404–420, doi:10.1100/tsw.2007.92.
[76] M. Lavagnino, A.E. Brooks, A.N. Oslapas, K.L. Gardner, S.P. Arnoczky, Crimp length decreases in lax tendons due to cytoskeletal tension, but is restored with tensional homeostasis, J. Orthop. Res. 35 (2017) 573–579, doi:10.1002/jor.23489.
[77] A. Herchenhan, N.S. Kalson, D.F. Holmes, P. Hill, K.E. Kadler, L. Margetts, Tenocyte contraction induces crimp formation in tendon-like tissue, Biomech. Model. Mechanobiol. 11 (2012) 449–459, doi:10.1007/s10237-011-0324-0.
[78] J. Zhao, X. Wang, J. Han, Y. Yu, F. Chen, J. Yao, Boost tendon/ligament repair with biomimetic and smart cellular constructs, Front. Bioeng. Biotechnol. 9 (2021), doi:10.3389/fbioe.2021.726041.
[79] J. Lin, W. Zhou, S. Han, V. Bunpetch, K. Zhao, C. Liu, Z. Yin, H. Ouyang, Cell-material interactions in tendon tissue engineering, Acta Biomater. 70 (2018) 1–11, doi:10.1016/j.actbio.2018.01.012.
[80] S.E. Szczesny, T.P. Driscoll, H.-Y. Tseng, P.-C. Liu, S.-J. Heo, R.L. Mauck, P.-H.G. Chao, Crimped nanofibrous biomaterials mimic microstructure and mechanics of native tissue and alter strain transfer to cells, ACS Biomater. Sci. Eng. 3 (2017) 2869–2876, doi:10.1021/acsbiomaterials.6b00646.
[81] D.C. Surrao, J.W.S. Hayami, S.D. Waldman, B.G. Amsden, Self-crimping, biodegradable, electrospun polymer microfibers, Biomacromolecules 11 (2010) 3624–3629, doi:10.1021/bm101078c.
[82] Y. Wu, Y. Han, Y.S. Wong, J.Y.H. Fuh, Fibre-based scaffolding techniques for tendon tissue engineering, J. Tissue Eng. Regen. Med. 12 (2018) 1798–1821, doi:10.1002/term.2701.
[83] J.M. Caves, V.A. Kumar, W. Xu, N. Naik, M.G. Allen, E.L. Chaikof, Microcrimped collagen fiber-elastin composites, Adv. Mater. 22 (2010) 2041–2044, doi:10.1002/adma.200903612.
[84] J.S. Shah, E. Palacios, L. Palacios, Development of crimp morphology and cellular changes in chick tendons, Dev. Biol. 94 (1982) 499–504, doi:10.1016/0012-1606(82)90366-9.
[85] N.S. Kalson, Y. Lu, S.H. Taylor, T. Starborg, D.F. Holmes, K.E. Kadler, A structure-based extracellular matrix expansion mechanism of fibrous tissue growth, Elife 4 (2015) e05958, doi:10.7554/eLife.05958.
[86] T.A.H. Järvinen, L. Jozsa, P. Kannus, T.L.N. Järvinen, M. Kvist, T. Hurme, J. Isola, H. Kalimo, M. Järvinen, Mechanical loading regulates tenascin-C expression in the osteotendinous junction, J. Cell Sci. 112 (1999) 3157–3166, doi:10.1242/jcs.112.18.3157.
[87] K.A. Hansen, J.A. Weiss, J.K. Barton, Recruitment of tendon crimp with applied tensile strain, J. Biomech. Eng. 124 (2001) 72–77, doi:10.1115/1.1427698.
[88] D.C. Stouffer, D.L. Butler, D. Hosny, The relationship between crimp pattern and mechanical response of human patellar tendon-bone units, J. Biomech. Eng. 107 (1985) 158–165, doi:10.1115/1.3138536.
[89] J. Diamant, A. Keller, E. Baer, M. Litt, R.G.C. Addidge, Collagen; ultrastructure and its relation to mechanical properties as a function of ageing, Proc. R. Soc. Lond. B (1972), doi:10.1098/rspb.1972.0019.
[90] K. Legerlotz, J. Dorn, J. Richter, M. Rausch, O. Leupin, Age-dependent regulation of tendon crimp structure, cell length and gap width with strain, Acta Biomater. 10 (2014) 4447–4455, doi:10.1016/j.actbio.2014.05.029.
[91] H. Fujie, Mechanical properties and biomechanical function of the ACL, in: M. Ochi, K. Shino, K. Yasuda, M. Kurosaka (Eds.), ACL Inj. Its Treat., Springer Japan, Tokyo, 2016, pp. 69–77, doi:10.1007/978-4-431-55858-3_6.
[92] S.G. McLean, K.F. Mallett, E.M. Arruda, Deconstructing the anterior cruciate ligament: what we know and do not know about function, material properties, and injury mechanics, J. Biomech. Eng. (2015) 137, doi:10.1115/1.4029278.
[93] C. Nelson, L. Rajan, J. Day, R. Hinton, B.M. Bodendorfer, Postoperative rehabilitation of anterior cruciate ligament reconstruction: a systematic review, Sports Med. Arthrosc. Rev. 29 (2021) 63, doi:10.1097/JSA.0000000000000314.
[94] P.P. Provenzano, R. Vanderby, Collagen fibril morphology and organization: implications for force transmission in ligament and tendon, Matrix Biol 25 (2006) 71–84, doi:10.1016/j.matbio.2005.09.005.
[95] E.A. Makris, R.F. MacBarb, D.J. Responte, J.C. Hu, K.A. Athanasiou, A copper sulfate and hydroxylysine treatment regimen for enhancing collagen cross-linking and biomechanical properties in engineered neocartilage, FASEB J. 27 (2013) 2421–2430, doi:10.1096/fj.12-224030.
[96] E.A. Makris, D.J. Responte, N.K. Paschos, J.C. Hu, K.A. Athanasiou, Developing functional musculoskeletal tissues through hypoxia and lysyl oxidase-induced collagen cross-linking, Proc. Natl. Acad. Sci. 111 (2014) E4832–E4841, doi:10.1073/pnas.1414271111.
[97] C. Frank, D. McDonald, J. Wilson, D. Eyre, N. Shrive, Rabbit medial collateral ligament scar weakness is associated with decreased collagen pyridinoline crosslink density, J. Orthop. Res. 13 (1995) 157–165, doi:10.1002/jor.1100130203.
[98] J.E. Marturano, J.D. Arena, Z.A. Schiller, I. Georgakoudi, C.K. Kuo, Characterization of mechanical and biochemical properties of developing embryonic tendon, Proc. Natl. Acad. Sci. 110 (2013) 6370–6375, doi:10.1073/pnas.1300135110.
[99] D.R. Eyre, M.A. Weis, J.-J. Wu, Advances in collagen cross-link analysis, Methods 45 (2008) 65–74, doi:10.1016/j.ymeth.2008.01.002.
[100] K. Reiser, R.J. McCormick, R.B. Rucker, Enzymatic and nonenzymatic cross-linking of collagen and elastin, FASEB J. 6 (1992) 2439–2449, doi:10.1096/fasebj.6.7.1348714.
[101] M. Lavagnino, M.E. Wall, D. Little, A.J. Banes, F. Guilak, S.P. Arnoczky, Tendon mechanobiology: current knowledge and future research opportunities, J. Orthop. Res. 33 (2015) 813–822, doi:10.1002/jor.22871.
[102] F.S. Passini, P.K. Jaeger, A.S. Saab, S. Hanlon, N.A. Chittim, M.J. Arlt, K.D. Ferrari, D. Haenni, S. Caprara, M. Bollhalder, B. Niederöst, A.N. Horvath, T. Götschi, S. Ma, B. Passini-Tall, S.F. Fucentese, U. Blache, U. Silván, B. Weber, K.G. Silbernagel, J.G. Snedeker, Shear-stress sensing by PIEZO1 regulates tendon stiffness in rodents and influences jumping performance in humans, Nat. Biomed. Eng. 5 (2021) 1457–1471, doi:10.1038/s41551-021-00716-x.
[103] W. Lee, H.A. Leddy, Y. Chen, S.H. Lee, N.A. Zelenski, A.L. McNulty, J. Wu, K.N. Beicker, J. Coles, S. Zauscher, J. Grandl, F. Sachs, F. Guilak, W.B. Liedtke, Synergy between Piezo1 and Piezo2 channels confers high-strain mechanosensitivity to articular cartilage, Proc. Natl. Acad. Sci. 111 (2014) E5114–E5122, doi:10.1073/pnas.1414298111.
[104] Y. Shen, Y. Pan, S. Guo, L. Sun, C. Zhang, L. Wang, The roles of mechanosensitive ion channels and associated downstream MAPK signaling pathways

in PDLC mechanotransduction, Mol. Med. Rep. 21 (2020) 2113–2122, doi:10.3892/mmr.2020.11006.
[105] G. Du, L. Li, X. Zhang, J. Liu, J. Hao, J. Zhu, H. Wu, W. Chen, Q. Zhang, Roles of TRPV4 and piezo channels in stretch-evoked Ca2+ response in chondrocytes, Exp. Biol. Med. Maywood 245 (2020) 180–189, doi:10.1177/1535370219892601.
[106] T. Ahsan, F. Harwood, K.B. McGowan, D. Amiel, R.L. Sah, Kinetics of collagen crosslinking in adult bovine articular cartilage, Osteoarthr. Cartil. 13 (2005) 709–715, doi:10.1016/j.joca.2005.03.005.
[107] E. Gineyts, O. Borel, R. Chapurlat, P. Garnero, Quantification of immature and mature collagen crosslinks by liquid chromatography–electrospray ionization mass spectrometry in connective tissues, J. Chromatogr. B 878 (2010) 1449–1454, doi:10.1016/j.jchromb.2010.03.039.
[108] J.E. Marturano, J.F. Xylas, G.V. Sridharan, I. Georgakoudi, C.K. Kuo, Lysyl oxidase-mediated collagen crosslinks may be assessed as markers of functional properties of tendon tissue formation, Acta Biomater. 10 (2014) 1370–1379, doi:10.1016/j.actbio.2013.11.024.
[109] X.S. Pan, J. Li, E.B. Brown, C.K. Kuo, Embryo movements regulate tendon mechanical property development, Philos. Trans. R. Soc. B 373 (2018) 20170325, doi:10.1098/rstb.2017.0325.
[110] J.M. Middendorf, M.E. Ita, B.A. Winkelstein, V.H. Barocas, Local tissue heterogeneity may modulate neuronal responses via altered axon strain fields: insights about innervated joint capsules from a computational model, Biomech. Model. Mechanobiol. 20 (2021) 2269–2285, doi:10.1007/s10237-021-01506-9.
[111] S.A. Park, I.A. Kim, Y.J. Lee, J.W. Shin, C.-R. Kim, J.K. Kim, Y.-I. Yang, J.-W. Shin, Biological responses of ligament fibroblasts and gene expression profiling on micropatterned silicone substrates subjected to mechanical stimuli, J. Biosci. Bioeng. 102 (2006) 402–412, doi:10.1263/jbb.102.402.
[112] G. Yang, R.C. Crawford, J.H.-C. Wang, Proliferation and collagen production of human patellar tendon fibroblasts in response to cyclic uniaxial stretching in serum-free conditions, J. Biomech. 37 (2004) 1543–1550, doi:10.1016/j.jbiomech.2004.01.005.
[113] R.K. Choi, M.M. Smith, J.H. Martin, J.L. Clarke, A.J. Dart, C.B. Little, E.C. Clarke, Chondroitin sulphate glycosaminoglycans contribute to widespread inferior biomechanics in tendon after focal injury, J. Biomech. 49 (2016) 2694–2701, doi:10.1016/j.jbiomech.2016.06.006.
[114] C.N.M. Ryan, A. Sorushanova, A.J. Lomas, A.M. Mullen, A. Pandit, D.I. Zeugolis, Glycosaminoglycans in tendon physiology, pathophysiology, and therapy, Bioconjug. Chem. 26 (2015) 1237–1251, doi:10.1021/acs.bioconjchem.5b00091.
[115] H.A. Benhardt, E.M. Cosgriff-Hernandez, The role of mechanical loading in ligament tissue engineering, Tissue Eng. Part B 15 (2009) 467–475, doi:10.1089/ten.teb.2008.0687.